Field and Airborne Spectroscopy Cross Validation—Some Considerations

Andreas Hueni, *Member, IEEE*, Alexander Damm, Mathias Kneubuehler, Daniel Schläpfer, and Michael E. Schaepman, *Senior Member, IEEE*

***Abstract*—Field spectroscopy is increasingly used in various fields of science: either as a research tool in its own right or in support of airborne- or space-based optical instruments for calibration or validation purposes. Yet, while the use of the instruments appears deceptively simple, the processes of light and surface interactions are complex to be measured in full and are further complicated by the multidimensionality of the measurement process. This study exemplifies the cross validation of *in situ* point spectroscopy and airborne imaging spectroscopy data across all processing stages within the spectroscopy information hierarchy using data from an experiment focused on vegetation. In support of this endeavor, this study compiles the fundamentals of spectroscopy, the challenges inherent to field and airborne spectroscopy, and the best practices proposed by the field spectroscopy community. This combination of theory and case study shall enable the reader to develop an understanding of 1) some of the commonly involved sources of errors and uncertainties, 2) the techniques to collect high-quality spectra under natural illumination conditions, and 3) the importance of appropriate metadata collection to increase the long-term usability and value of spectral data.**

***Index Terms*—Calibration, information systems, radiometry, spectroscopy.**

I. Introduction

FIELD spectroscopy is a combination of technology and methodology that has been applied for several decades to obtain information about reflective properties of materials under field conditions [1]. Field spectrometers have been proliferated in the past decade and many researchers have started to use these instruments and their data to answer a plethora of scientific questions, at first often neglecting the involved intrinsic complexities of the spectroradiometric data acquisition. The handling of these devices is deceptively simple and yet the acquisition of reliable spectral data is a demanding affair [2] requiring a great deal of experience to minimize biases that can be easily introduced. This contrasts with the fact that *in situ* spectral data are often used to validate airborne and satellite data and are commonly referred to as ground truth [3]. There is in fact no such thing as ground truth; it is at best an unbiased traceable representation of the true value with an associated uncertainty [4]. It is also a common misperception that expensive and freshly calibrated field equipment delivering a large number of spectral bands is by default providing a more truthful picture of the environment than airborne- or space-based instruments [5]. Not only is the acquisition of spectral field data prone to errors, but the acquired information is also usually at a scale different from the airborne- or space-based data, and, thus, not easily compared [2], [5], [6]. Consequently, cross validation of *in situ* and air- and space-borne spectroscopy data requires a detailed understanding of the measurement process, the involved scales and scattering mechanisms, and the processing applied to the data at various processing levels.

Although field spectroscopy predates the development of air- and space-borne imaging spectrometers by many years, both technologies have the common goal of acquiring accurate data on the spectral reflectance and properties of Earth surface materials from a remote location [1]. Distinct methodologies are necessary 1) to acquire spectral properties of both individual elements (e.g., leaves, minerals) and spatial assemblages of the Earth's surface (e.g., vegetation canopies) [1], 2) to obtain reflectance factors as input to models (surface reflectance models or process-based models of the Earth's surface and atmosphere) [1], and 3) for the vicarious calibration of airborne- and space-based remote sensing devices, as well as the validation of derived surface variables [1], [7]. Even nowadays, field spectroscopic measurements suffer from the absence of consistent protocols and procedures, an essential requirement for high-quality data with stated levels of accuracy and uncertainty [1], [7], [8]. A comprehensive approach holding together guidelines and best practices in field data acquisition is still not defined with sufficient maturity [8].

Since spectroradiometric measurements still remain one of the least reliable of all physical measurements [9], [10], close

Manuscript received April 9, 2016; revised June 10, 2016 and July 12, 2016; accepted July 20, 2016. Date of publication October 3, 2016; date of current version February 13, 2017. The APEX sensor model was developed with support from the EURAMET EMRP ENV-04 and ENV-53 Projects. The EMRP was supported in part by the EMRP participating countries within EURAMET and the European Union. Panel cross-calibration results and error budgets due to manual reference panel alignment presented in this study were collected during a COST OPTIMISE ES1309 training school. This work was also supported by the University Research Priority Program on "Global Change and Biodiversity". The work of A. Damm was supported by a grant of the Swiss University Conference and ETH-Board in frame of the KIP-5 Project Swiss Earth Observatory Network and by a grant of the European Space Agency in frame of the FLEX-BRIDGE study (ESA RFP IPL-PEO/FF/lf/14.687). *(Corresponding author: A. Hueni.)*

A. Hueni, A. Damm, M. Kneubuehler, and M. E. Schaepman are with the Remote Sensing Laboratories, University of Zurich, Zurich 8057, Switzerland (e-mail: ahueni@geo.uzh.ch; adamm@geo.uzh.ch; kneub@geo.uzh.ch; schaep@geo.uzh.ch).

D. Schläpfer is with ReSe Applications, Wil 9500, Switzerland (e-mail: daniel@rese.ch).

Color versions of one or more of the figures in this paper are available online at http://ieeexplore.ieee.org.

Digital Object Identifier 10.1109/JSTARS.2016.2593984

attention must be paid to the reproducibility of remote-sensing methodologies [11]–[13]. Reproducibility is dependent upon uncertainties in the spectral measurement that themselves are caused by various sources of variability [14]. A study designed to quantify uncertainty in field measurements of vegetation canopy hemispherical conical reflectance factors (HCRF) [14] (for terminology see [15]) found sources of measurement variability due to 1) instrument characteristics [16], [17], 2) irradiance anisotropy [18]–[20], and 3) measurement methodology due to target complexity, where uncertainty is linked to the sensor resolution defined by the instantaneous field of view (iFOV) and spatial variation of target properties (natural variability) [1], [7], [21]. Spatial nonuniformity across the sensor field of view (FOV) and the difficulty to accurately determine the actual measurement support are further sources of measurement uncertainty [22].

The goal of this paper is to identify and exemplify cross-validation strategies for *in situ* point spectroscopy and airborne imaging spectroscopy data and to introduce and quantify sources of uncertainties that affect such validations. This is achieved by 1) summarizing fundamental physical quantities involved in spectroscopy, 2) providing an overview of the current state of the art–of-field spectroscopy by compiling best practices of data collection evolved over the past decades, as well as 3) expanding on the general constraints of airborne spectroscopy data acquisition and processing. The establishment of a fully propagated uncertainty budget is beyond the scope of this study, and, hence, information regarding biases and uncertainties is derived from a case study and indicates quantitative ranges that may be expected. This forms the basis to appreciate the importance of data quality assessment and the difficulties involved with cross-validation strategies of *in situ* and airborne spectroscopy data at various processing levels within the spectroscopy information hierarchy. The case study exemplifies data collection, processing and validation strategies that can be applied within such an integrated approach based on the operational interaction of components of *in situ* and airborne spectrometer processing and information systems. Remote sensing of vegetation is emphasized in parts of this study, as the case study uses data from a measurement campaign involving crops and pastures; however, the general concepts are generically applicable and quite independent of target types.

II. Fundamentals of Spectroscopy

A. Physical Quantities in Spectroscopy

Acquired spectroscopy data progress typically through processing levels from raw to derived products [23] (see Fig. 1). According to the information theory, the higher the processing level, the more meaningful the data [24], [25], and, consequently, the higher the number of potential users. The processing levels of airborne imaging spectrometers and ground-based non-imaging spectrometers are essentially identical. Level 0 holds raw digital numbers (DNs), level 1 refers to radiometrically calibrated data, level 2 comprises reflectance factors of a usually hemispherical-conical beam geometry, which may differ depending on the instrument setup and the radiance to reflectance

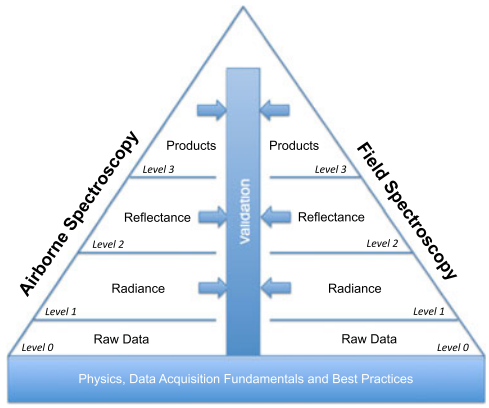

Fig. 1. Spectroscopy information hierarchy showing acquisition and processing stages of airborne- and ground-based spectroscopy data, their common base of physics and measurement principles, and their cross validation as described in this paper.

factor conversion algorithm, and level 3 incorporates derived biogeophysical information, for example, estimated vegetation properties.

1) Level 1: Irradiance and Radiance: According to the four stream theory of Verhoef [26] and Verhoef and Bach [27], irradiance (*E*) incident on a given surface consists of two fluxes, E^{dir}, representing the downward flux that is directly transmitted between top-of-atmosphere and the surface, and E^{dif}, representing the diffuse downward flux and the diffuse upward flux reflected back from the atmosphere.

E^{dir} of a Lambertian and flat surface (i.e., without topography effects) can be described as a function of the extraterrestrial solar irradiance (E^0), direct transmittance of the atmosphere for sunlight (τ_{ss}), and the cosine of the illumination zenith angle θ_{il}, with

$$E^{\mathrm{dir}} = \tau_{\mathrm{ss}} E^0 \cos\theta_{\mathrm{il}}. \tag{1}$$

The cosine of θ_{il} is defined as

$$\cos\theta_{\mathrm{il}} = \cos\theta_n \cos\theta_s + \sin\theta_n \sin\theta_s \cos(\varphi_n - \varphi_s) \tag{2}$$

where θ_s, φ_s are the zenith and azimuth angle of the sun rays and θ_n, φ_n are the zenith and azimuth angle of the surface normal vector.

E^{dif} of a Lambertian and flat surface under a specific sun position and status of the atmosphere can be approximated as a function of the diffuse transmittance of the atmosphere for sunlight (τ_{sd}) and the spherical albedo ρ_{dd}, characterizing the multiple reflection of E between the target and its surroundings and the atmosphere. E^{dif} can be accordingly expressed as

$$E^{\mathrm{dif}} = \frac{\tau_{\mathrm{sd}} + \tau_{\mathrm{ss}} \overline{r_{\mathrm{sd}}} \rho_{\mathrm{dd}}}{1 - \overline{r_{\mathrm{dd}}} \rho_{\mathrm{dd}}} E^0 \cos\theta_{\mathrm{il}} \tag{3}$$

where $\overline{r_{\mathrm{sd}}}$ is the spatially homogenized directional-hemispherical reflectance of the surroundings, and $\overline{r_{\mathrm{dd}}}$ is the spatially homogenised bihemispherical reflectance (BHR) of the surroundings (cf., Schaepman-Strub *et al.* [15] for a definition of used terminology). The expression of E^{dif} under natural irradiance conditions (i.e., anisotropic diffuse irradiance) is more complicated (cf., [28]).

The directional radiance signal leaving a tilted hemispherically-illuminated surface measured at surface level (L) can be expressed as

$$L = \frac{r_{\mathrm{so}} \cdot E^{\mathrm{dir}} + r_{\mathrm{do}} \cdot E_t^{\mathrm{dif}}}{\pi} \tag{4}$$

where r_{so} is the bidirectional reflectance factor of the target and r_{do} is the hemispherical directional reflectance factor (HDRF) of the target, E^{dir} is the direct, and E^{dif} is the diffuse sky radiation.

2) Level 2: Reflectance Quantities: The general lack of standardization in application of reflectance terminology leads to uncertainties in data reporting and interpretation [1], [14], [15]. Field reflectance measurements can geometrically be described as HCRF, although they are sometimes referred to as HDRF when the instrument has a very narrow FOV (e.g., 3° or less) [1]. It is to be noted that this definition deviates from the original definitions by Nicodemus [29], where the terms HDRF and HCRF were strictly referred to a perfectly isotropic (i.e., diffuse) irradiance field. A detailed discussion pertaining to principles of field measurements of reflectance factors can be found in [30] and [31]. Due to the angular (anisotropic) distribution of irradiance in the field environment, measured HCRF is subject to uncertainty introduced by the irradiation environment and may, therefore, not be solely related to properties of the surface [1], [19]. In addition, temporal variations in anisotropic hemispherical illumination (varying solar zenith angles) and temporally varying atmospheric conditions lead to variability in field measured HCRF [19], [28]. Such uncertainties can only be eliminated given identical illumination conditions for both target surface and incoming radiation measurements.

Since HCRF measurements are dependent on the sensor viewing angle and illumination scenario, derived biogeophysical variables (Level 3 products) can strongly vary with changing data acquisition geometry, as could, for example, be shown in studies on angular sensitivity of vegetation indices from multi-angular, field [28], [32], [33], and space-based data [34].

3) Level 3: Biogeophysical Variables: Absorption, transmission, and reflectance are the main processes describing the interaction of photons with the atmosphere-surface system. These processes are determined by properties of the atmosphere (e.g., the aerosol load, atmospheric water vapor) and the surface (e.g., composition of biochemical constituents in vegetation, soil wetness, or snow impurities). Measurements of light that previously interacted with either the atmosphere or the surface or both carry information of these properties and can be used to retrieve them [35]. The commonly used top-of-canopy approach applies an atmospheric correction to minimize the impact of atmospheric absorption and scattering effects on measured radiance data and to eventually obtain HCRF data. Assumptions applied during the atmospheric correction (i.e., Lambertian surface reflectance as simplification of reflectance anisotropy, simplifications of irradiance anisotropy, and the fractional amount of diffuse and direct irradiance components, layering of aerosols, or fixed aerosol phase functions) likely alter the reliability of HCRF calculations [28]. Particularly for vegetation, canopy structure was found to impact retrieval accuracy of biogeochemical vegetation properties, e.g., chlorophyll or water content [28], [36].

The retrieval of atmospheric or surface variables requires detailed understanding about the physical processes describing the photon–atmosphere or photon–surface interactions [37], [38]. Furthermore, sensor properties (e.g., spectral resolution, signal-to-noise ratio) are known to determine the information content and quality of the measured signal, thus complicating the reliable extraction of biogeophysical variables [17]. Nowadays, a comprehensive set of analytical tools exists to facilitate the retrieval of atmospheric or surface variables. The various approaches to extract biogeophysical variables from HCRF data range from simple empirical-statistical approaches to rather complex physical-based approaches that combine observations with process models and techniques of data assimilation [39]. The latter invert vegetation radiative transfer models (RTM) such as the commonly applied models PROSPECT [40] and SAIL [41]. Common to all methods is the requirement to cope with and minimize the impact of all aspects previously mentioned to eventually retrieve precise and accurate bio-geophysical variables [35], [42]. Further, all algorithms subsequently applied to the data within the information hierarchy may add their own biases and uncertainties, entailing that errors occurring in lower processing levels are propagated, rendering higher level data more biased and uncertain.

B. Data Acquisition Approaches and Processing Stages

1) General Data Acquisition Considerations: Spatial sampling considerations are important to account for the natural variability of measured targets. Several studies discuss the variability of field spectroscopic measurements with varying sensor altitude (either defined as *height above sea level* or *above site* [1], as *distance to target* [7], or as *altitude above the vegetation surface* [14], [21]), where the methodological uncertainty is linked to the sensor iFOV and the spatial variations in target properties. It was shown for row crops that variance of reflectance factor measurements from nadir at low altitudes was caused by row effects, which disappeared at higher altitudes [7], [21]. Milton *et al.* [1] state that the operator should seek to ensure that field measurements characterize variations of the inherent properties of the surface, and not positional variations in the location of the device; otherwise, methodological uncertainties are likely to cloud the assessment of temporal and spatial trends [14].

The design of representative sampling schemes is challenged by the individual spatial length scales of biogeophysical variables [43]. A spatial length scale describes the degree of spatial dependence of a variable and can be derived by variogram analysis, representing the variance of a biogeophysical variable as function of spatial distance. Consequently, a statistically sound comparison of ground and airborne data relies on sampling schemes specifically optimized for individual surface variables.

The selection of appropriate sampling schemes can be arbitrarily complex, for example, in the case of complex structured canopies (i.e., rows of crops such as olives or vineyards), where altering fractions of plant and background are observed by a

remote sensor. Optical measurements from airborne platforms provide spatially continuous measurements and allow assessing the spatial heterogeneity of surface variables. Imaging spectroscopy data can, thus, be used to inform field-sampling strategies. Sampling approaches [8] and methodologies to assess the necessary number of samples in the field to characterize a surface have been reported in the literature [21], [43].

Temporal considerations are also important as they determine the representativeness and accuracy of spectroscopic measurements. Reflectance characteristics of vegetation canopies, for example, can change in a short time due to physiological adaptation, yielding changes in biochemistry (e.g., pigment contents [44] and water content [45]) or structure (e.g., leaf angle and related to this, changing visibility of upper and lower leaf surfaces [46]).

2) Field Spectroscopy Data: Various studies have discussed general guidelines on field spectroscopy techniques and data processing, ranging from campaign planning to measurement collection and data management [8], [47]. They defined experiments to assess the reproducibility of field measurements [11], [12], to derive field standard uncertainties [14], and highlighted the importance of common protocols to ensure long-term value of field spectroscopic data [1]. Field data collection should take into account important issues of field spectroscopic data acquisition and include associated metadata to ensure the measured quantities are, ideally, made traceable with associated combined uncertainties, and, thus, as close to the notion of *ground truth* [sic] as possible.

Milton *et al.* [1] identified a growing interest among field spectroscopy data users in measuring *radiance quantities* in the field instead of reflectance factors, stating that "*the dominant paradigm of field spectroscopy is based on relative measurements, in which the radiance of the target is compared with that of a reference panel.*" Given that the instrument has a linear response and the reference panel is accurately calibrated, absolute radiance calibration of the instrument is not essential. Radiance calibrated field spectrometers, however, provide more information on the radiation environment in which the measurements take place [1]. As such, the primary (radiance) measurements are expressed in SI (Système International d'Unités) units and are, therefore, traceable to international standards.

Measuring incoming radiation is generally performed using calibrated reference panels, which are neither perfectly reflecting nor perfectly diffuse and both of these properties vary with wavelength [48], [49]. Reference panels must be carefully levelled (e.g., by using a tripod and a bubble level) and care must be taken to completely fill the FOV of the spectroradiometer [1], [30].

Temporal variations in anisotropic hemispherical *illumination characteristics*, solar zenith angle changes, and atmospheric scattering introduce uncertainties in field spectroscopic measurements [14]. According to Goetz [47], the interval between reference measurements on a clear day is a function of the rate of change in the solar elevation angle. If the atmosphere is unstable, reference measurements should be taken just before and after each target measurement, thus minimizing the time gap between target and reference panel (incoming radiation) measurements [2]. Data acquisition is ideally performed within 2 h of local noon [47]. The radiometric consistency of a diurnal dataset can be checked by analyzing reference panel radiance time series. In an ideal case, these radiances should follow a trajectory given by the cosine of the sun zenith angle. Deviations of this theoretical curve must then be the result of either unstable illumination conditions or measurement process related issues such as angular errors in the horizontal panel alignment, spectral contamination, or instrument biases.

Thorough consideration must be paid to the *measurement geometry* for field spectroradiometric measurements [1]. The reproducibility of repeated measurements over the same point profits from a fixed frame or various types of support (e.g., tripod, mast, tower, tramway). Nearby objects cause spectral radiance errors in the field measurements [47], [50]. Goetz [47] found that wearing dark clothes does not mitigate the effects of proximity to the measured sample as much as the right choice of cloth fabric (i.e., cotton instead of polyester). The least effect of the operator was found when measurements were made perpendicular to the solar principle plane, while keeping at least 1-m distance from the measurement support minimized the contribution from scattered radiation off the clothing and made skylight obscuration negligible [47].

Instrument uncertainties are a further reason affecting field spectroscopic measurements. Laboratory-based instrument uncertainty characterizations were found to significantly differ from field-derived uncertainties and must be interpreted with care [14]. The difficulty to accurately determine the actual measurement support of a sensor, as well as the spatially nonuniform responsivity across the sensor FOV, were found to add measurement uncertainties especially in spatially complex targets [22]. Besides accurate instrument calibration, temperature effects are a problem with many field spectroradiometers, especially when using multiple detectors [5], [51]. For ASD spectroradiometers, it is recommended to start the device at least 30 min prior to measurements to thermally stabilize it, although reaching a thermal equilibrium may take more than 1 h [1], [5], [14], [51]. Some instruments allow the configuration of internal averaging, designed to reduce the noise of the signal, while other approaches apply averaging in postprocessing to estimate the noise for quality control purposes [5].

The importance of *common standards and protocols* when performing field spectroscopic measurements is being increasingly recognized and has been emphasized in the recent literature [1], [7], [14], [30], [52]. The measurement conditions should be accurately documented by a set of metadata, following formalized standard guidelines [1], [8]. Spectral databases like SPECCHIO [53], supporting the storage of such comprehensive metadata, are an important step toward expanded discovery, data-mining, and long-term reusability of field spectral measurements [54]. A list of metadata variables implemented in SPECCHIO can be found in the literature [8], [53], while the most recent information can be obtained from either the SPECCHIO application help or web site [55].

3) Airborne Spectroscopy Data: Airborne data acquisitions are most often a tradeoff between ideal sampling patterns, ground resolution, and monetary/temporal restrictions. De-

pending on the study, flight lines might be optimized for reflectance anisotropy effects, either to enhance or suppress them as much as possible. This may, however, be contradictory to the flight pattern delivering the whole dataset in the shortest possible timeframe. Optimizing the temporal aspect should be considered important if the phenomena to be observed change significantly over time, e.g., due to melting processes for snow or water fluxes in tidal regions, or if funds are limited and the introduction of additional flight lines might result in greater costs. In pushbroom sensors like the Airborne Prism EXperiment (APEX) [56], pixel sizes in across-track direction are given by the above-ground altitude of the sensor while along-track dimensions are driven by aircraft ground speed and integration time per scan line. In practice, pixels are never square but either stretched or compressed in along-track direction. Square pixels are the result of georectification, which introduces additional uncertainties due to spatial resampling [57].

Ideally, airborne spectrometers are regularly calibrated radiometrically, geometrically, and spectrally in specialized laboratories [58], making them traceable to SI units. Acquired raw data are calibrated to radiance units by applying calibration factors. To achieve the highest degree of accuracy, the data processing must implement a detailed sensor model that can be inverted to compensate for specific sensor characteristics, such as pressure or temperature behavior impacting the radiometric, geometric, or spectral performance of the instrument during flight operations [59].

The raw geometry and acquisition time of every pixel is given by the smoothed best estimate trajectory (SBET) information produced from data recorded by an inertial measurement unit coupled with a GPS receiver [60]. SBET data are used to define the 3-D position of each pixel in combination with a digital elevation model. This 3-D information is subsequently used during atmospheric correction and georectification. Positional accuracies are influenced by the accuracy of the raw positional data, the resolution and accuracy of the elevation model, and the boresight calibration, the latter being specific for each instrument build-in into the carrier platform.

4) Spectroscopy Data Processing Stages: The physical quantities present in the spectroscopy information hierarchy were introduced in Section A. The related processes commonly applied to spectroscopy data are briefly described hereafter with further information given in the methods section related to the case study. The reader may also wish to refer to the detailed processing and dataflow diagram provided in Fig. 2, denoting the processing modules and dataflow as applied within the case study of this paper.

Airborne imaging spectrometer data are typically stored and processed within processing and archiving facilities (PAF), comprising integrated hardware and software components for data storage and processing [60]. Ground-based point spectroradiometer data are ideally handled by spectral databases in combination with processing algorithms, for example, the SPECCHIO spectral information system [61], [62].

Radiometric calibration relies on calibration coefficients usually established under laboratory conditions that establish a link between at-sensor radiances and recorded DNs [63]. During data calibration, DNs measured by spectroradiometers are converted to radiance values by applying coefficients supplied by the instrument manufacturer or directly by a calibration laboratory.

At-sensor radiance data of airborne imaging spectrometers are typically converted to bottom of atmosphere HCRFs by employing atmospheric correction algorithms. The process generally involves the modeling of irradiance for each individual pixel to compensate for effects due to the state of the atmosphere (i.e., transmission, path scattering, and adjacency). The pixel HCRF is then calculated from corresponding radiance measurements and irradiance estimates.

Field spectroradiometer-based target HCRFs are computed from target radiances, and measurements defining the irradiance, such as given by white reference panel radiances and panel reflective properties, or cosine receptor-based irradiances.

Product generation may involve a great variety of algorithms depending on the intended application. In addition, product generation may be based on HCRF data or use radiance data when employing coupled model approaches [64].

5) Vicarious Validation: Besides on-board calibration approaches, vicarious validation provides an alternative and independent way to evaluate the performance of sensors in flight. Usually, *in situ* measurements and corresponding at-sensor signals are compared and the degree of agreement of both signals indicates the in-flight sensor performance. However, vicarious validation is essentially possible across all levels of the spectroscopy information hierarchy (see Fig. 1). According to Anderson and Milton [11] and Kriebel [18], several vicarious calibration/validation strategies are typically applied, namely *radiance-, irradiance-,* and *reflectance-based methods* [65]–[67]. An optional *multitarget reflectance-based vicarious calibration* approach as, e.g., implemented in ATCOR4 [68], [69] is based on a set of reference targets that characterize homogeneous and flat areas of a minimum extent of 10×10 m, covering a large dynamic range of radiance values. This approach holds the potential to even evaluate a possible nonlinear behavior of the sensor.

The *radiance-based validation* is used to check the accuracy of the measured at-sensor radiance values of a remote sensing system during in-flight conditions. It relies on an accurate calibration of the sensor system to physical units, (e.g., to mW/(m^2 sr nm)) [70]. These data are to be compared to the output of radiative transfer calculations, requiring accurate geometrical inputs for sensor and sun positions and angles as well as reference data of ground HDRF, often approximated by in field HCRF measurements. The state of the atmosphere is to be characterized independently from the image data by means of sun photometer measurements, i.e., by inversion of the irradiance field on the ground. Accordingly, modeled data may still be significantly biased by adjacency effects, which cannot easily be quantified from ground measurements. Due to this, the validation accuracy is better for low flight altitudes, negligible topography, and for large uniform targets used as references. It may be further improved by dedicated measurements of adjacency radiance, i.e., the angular diffuse irradiance, and by incorporation of appropriate models for irradiance distribution [71].

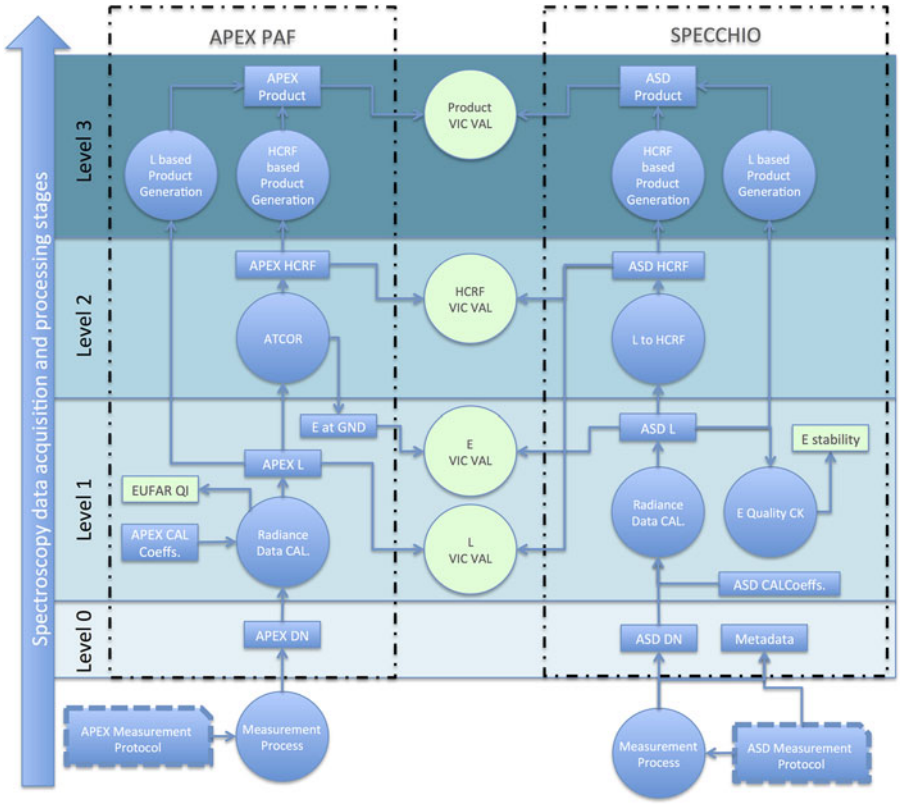

Fig. 2. Spectroscopy information hierarchy showing acquisition and processing stages of airborne- and ground-based spectroscopy data and their interrelations with the processing modules and data flow as applied within the case study of this paper.

The *irradiance-based validation* is mainly a validation of the atmospheric compensation process and the underlying RTM in comparison to irradiance values measured on ground.

The output of the atmospheric compensation is comparable to bottom of atmosphere in field HCRF, which may be used for *reflectance-based validation*. The variations of reflectance anisotropy within the typical observation angle of airborne instruments of 0.5–1 mrad are in practice negligible (i.e., below 0.2%, if an extreme BRDF variation with factor 2 is assumed within an angle of 60°). Therefore, bottom of atmosphere HCRF is considered a directional rather than a conical quantity, i.e., variations of the BRDF within the conical FOV of airborne data are irrelevant for data processing and analysis. Variations of in field HCRF acquired by field spectroradiometers are significant. However, the difference in observation angle (i.e., the conical nature of field data acquisitions) is typically not corrected for under the assumption that reflectance anisotropy induced variations acquired with a $\leqq 8°$ FOV of a field spectrometer are a sufficiently close approximation of the directional assumption.

A further conceptual difference between in field measurements and airborne data is the reflectance quantity itself. The data derived from airborne data are *reflectances* in a strict sense: the HDRF is calculated by relating the modeled irradiance per pixel to the bottom of atmosphere radiance after accounting for all the above-mentioned atmospheric effects. The inversion of the radiative transfer equation requires atmospheric parameter retrieval of water vapor and aerosols and one iteration to account for adjacency effects [72]. The field data, on the other hand, are *reflectance factors* as they are related to a measurement of a white reference panel; they are absolute reflectance factors if corrected for the reference panel reflectance [15].

To overcome the limitation of reflectance anisotropy-induced variations, the reflectance-based validation would optimally be done on the level of BHR values, i.e., the spectral white sky albedo. The airborne HCRF data may be corrected to BHR by an appropriate model describing the underlying reflectance anisotropy [31]. The same applies to field data. A precondition to this would be the multiangular *in situ* data acquisition by goniometers [33], [73] and the correct conversion of these multiangular measurements to BHR values, taking into account the sun position during field measurements as the principal irradiance direction [74].

Vicarious validation approaches are distinguished based on the instrument or method to be evaluated and on the quantity that is compared. The major problem common to all cases is consistency in geometrical, but also spectroradiometrical sense. It is not only the spatial resolution which is significantly different between single point surface measurements and airborne measurements, but also the differences in observation angles, which, in combination with reflectance anisotropy, can lead to significant errors. For the spectroradiometric part, it all comes down to a consistent calibration for both the spectral and the radiometric response, such that physical quantities measured on ground and from an air- or space-borne instrument

TABLE I
OVERVIEW OF VALIDATION LEVELS FOR THE USE OF FIELD SPECTROSCOPY IN SUPPORT OF IMAGING SPECTROSCOPY DATA

Level/Parameter	Field Spectra	Airborne Spectra	Model	Use
Level 1 *At-sensor radiance*	HCRF adapted to sensor properties input to RTM	Calibrated at-sensor radiances	Forward atmospheric RTM	Airborne Sensor calibration/validation
Level 1 *Total ground irradiance*	Total irradiance measurements	None	Irradiance model in atmospheric RTM	Irradiance model and ground sensor validation
Level 2 *Bottom of atmosphere HCRF*	HCRF values	Atmospherically compensated HCRF	Atmospheric compensation via inverse RTM	Airborne HCRF validation
Level 2 *Bottom of atmosphere BHR*	BHR derived from multiangular ground measurements	Atmospherically compensated and reflectance anisotropy corrected BHR	Atmospheric compensation and reflectance anisotropy correction	In-depth validation of correction models
Level 3 *Products*	Surface variables derived from field HCRF	Surface variables derived from airborne HCRF	Various atmosphere-ground coupled models	Surface variable validation

are comparable. An overview of the various approaches is given in Table I.

III. CASE STUDY—DATA AND METHODS

A. Study Site

The Oensingen test site (47°17′11″N, 7°44′01″E, 452 m above sea level) is an agricultural area located near the village of *Oensingen* in the Swiss midlands. The orographically flat site is characterized by small agricultural fields with grassland, clover fallow cropping, bean, maize, rapeseed, pea, sugar beet, and winter wheat as dominant crops. The test area is equipped with an eddy-flux tower and is frequently surveyed in the framework of field and airborne campaigns.

B. Airborne Data

APEX is a pushbroom imaging spectrometer featuring visible and near-infrared (VNIR) and shortwave infrared (SWIR) channels with a common fore optic [56]. Both channels record 1000 spatial pixels in across-track direction with the ground resolution being a function of aircraft above ground level altitude and of the field of view of 28°. Resulting on-ground pixel sizes are typically in the range of 1.5 to 2.5 m. VNIR and SWIR channels are spectrally overlapping in the near infrared and cover wavelengths ranges of 372–1015 and 940–2540 nm, respectively, [75] with the VNIR channel allowing spectral hardware binning of its 334 spectral bands, by default resulting in 114 VNIR bands. Detailed system characteristics of APEX are covered in Schaepman *et al.* [56].

APEX imaging spectrometer data were obtained within a single flight line in north-south direction on the 17th June, 2009 starting 1044 UTC and taking 4 min to complete. The sensor altitude was 5150 m above sea level resulting in an across-track pixel size of 2.5 m with a geolocation accuracy of 1 to 2 pixels. Raw data were calibrated to radiances within the APEX PAF [60], [76], [77], corrected for the effects of spectral shifts on radiometry for both VNIR and SWIR channels [59], and resampled to standardized centre wavelengths to remove spectral misregistrations. These data calibration steps utilized coefficients calculated within the APEX Calibration Information System [58] based on calibration data acquired in the APEX Calibration Home Base (CHB) [78]. The APEX PAF generated quality layers and quality metadata are compliant with generic quality indicators elaborated within EUFAR HYQUAPRO [79].

Level 1 data were converted to HCRF data using the MODTRAN5 [80] based atmospheric correction software ATCOR4 [68], [69]. Spectral polishing using a derivative approach [72] was applied to remove remaining spectral artefacts in the ATCOR4 reflectance outputs.

ATCOR4 calculates the irradiance for each pixel, utilizing a digital terrain model to include slope, aspect, sky-view factor, and adjacency effects [69]. Atmospheric water vapor and aerosol characteristics are derived from the radiance data to account for both atmospheric transmittance and scattering effects. The irradiance calculation of ATCOR4 combines the directly transmitted solar irradiance with the diffuse irradiance produced due to scattering by aerosols and molecules of the atmosphere [72]. Scattering involves single scattering by aerosols, but also multiple scattering interactions with the surrounding area and its reflective properties. Consequently, the contribution of adjacency effects is included in the calculation, also considering direct irradiance stemming from adjacent terrain. All adjacency effects assume a Lambertian behavior of adjacent areas. ATCOR4 produces a spectral data cube containing the per-pixel direct and diffuse irradiance, which may then be compared to *in situ* white reference panel measurements.

Inverting the MODTRAN5 radiative transfer code leads to a surface reflectance quantity very much similar to an HCRF measured in the field at the same geometrical solar incidence angles and observation conditions. The major difference is the very small observation angle of one pixel, i.e., iFOV. ATCOR4 reflectance products for an iFOV $<< 0.03°$ are in a strict sense HCRF data but are often and well approximated as HDRF [15].

HCRF data were georectified using PARGE [81]. The topographic correction within ATCOR4 and PARGE was based on the swissALTI3D digital elevation model with a 2-m grid cell size provided by the Swiss Federal Office of Topography (*swisstopo*).

C. Field Spectroscopy Data

Field spectroscopic measurements were carried out using an ASD FieldSpec Pro high-resolution spectroradiometer (PAnalytics, CO, USA) on the 16th and 17th June, 2009 to support vicarious validation and to derive vegetation information. The

ASD registers reflected radiation within the spectral range of 350–2500 nm with a nominal bandwidth of 3 nm between 350 nm and 1000 nm and 10 nm between 1000 and 2500 nm. The nominal FOV of the instrument is 25°. A calibrated Spectralon white reference panel (0.25 m × 0.25 m) mounted on a tripod and adjusted horizontally using a bubble level was used to measure incident irradiance.

For this case study, we selected two sets of targets. The first set comprises six artificial and natural targets to facilitate the evaluation of Level 1 and Level 2 data. The rationale was to include surfaces covering a wide dynamic range of radiance values. The second set of targets comprises 12 homogeneous crop fields to evaluate the agreement of vegetation information derived from both field and airborne spectroscopy data. The term "*fields*" refer to agricultural parcels covered by a specific crop type.

The measurement setup was adapted to characterize surface areas of about 2.0 m^2 in a homogeneous surrounding to match the APEX pixels size and the average geolocation accuracy of 1–2 pixels. The instrument's fibre optic was used in nadir view approximately 1 m above the surface. Between 20 and 30 individual measurements were recorded moving the fibre optic manually over the surface, bracketed by five spectra of a white reference panel. The integration time was automatically optimized in order to maximize the signal-to-noise ratio.

The ASD binary files were imported into a SPECCHIO instance including automatic calibration from DN to radiance, and augmented with metadata (e.g., spatial position, target name, sensor, and sun geometry) to assist the automated computation of validation data. The final metadata space [82] for this study comprised 30 metaparameters.[1] The preprocessing of the measured radiance signals consisted of evaluating the measurement uncertainty through the analysis of white reference panel spectra, correcting for radiometric miscalibration, in particular for in-between detector jumps at 1000 and 1800 nm, due to sensitivity drifts caused by temperature using a multiplicative instrument model [5], [51].

The reference panel readings bracketing the target spectra were linearly interpolated over time for each spectral band to provide a best estimate of the solar irradiance for each target radiance spectrum. Target HCRFs were computed using the interpolated irradiance, including a compensation for the reflective properties of the reference panel. Measured radiance, irradiance, and derived HCRF data were directly used for the vicarious validation approach.

D. Algorithm Implementation

Most algorithms for data quality checks were implemented in MATLAB and written in a generic way to allow their application to other datasets as well. An underlying and powerful feature is the direct connection from MATLAB to the SPECCHIO system, giving full access to the metadata space. Spectral data and metadata for all plots involving *in situ* spectra shown in this study were automatically selected from SPECCHIO, loaded into MATLAB, processed and plotted ready for production. Selection of targets to be involved in the analysis was done interactively using the SPECCHIO spectral data hierarchy browser component.[2] Exceptions to this are the biogeophysical variables retrieved by model inversion, which was not yet fully integrated with either SPECCHIO or the APEX PAF.

E. Biogeophysical Variable Retrieval

One commonly used vegetation index and three vegetation variables were exemplarily investigated to quantitatively assess the agreement of Level 3 data products derived from simultaneously acquired *in situ* and airborne-based HCRF data. These are the normalized difference vegetation index (NDVI), the canopy chlorophyll content (cCAB), canopy water content (cCW), and leaf area index (LAI). The NDVI is widely used in vegetation remote sensing and was designed as proxy of vegetation health and structure [83], [84]. For this specific study, NDVI was calculated for both *in situ* and APEX data using narrow band implementations [85] after spectrally convolving the *in situ* HCRF spectra to APEX bands as

$$\mathrm{NDVI} = \left(R_{800.1} - R_{671.4}\right) / \left(R_{800.1} + R_{671.4}\right) \qquad (5)$$

where R_x is the reflectance factor at the given APEX centre wavelength in nanometers.

The three vegetation variables are important plant traits and characterize the biochemical (cCAB, cCW) and structural (LAI) state of vegetation canopies [86], [87]. All three variables were obtained from HCRF data using a model inversion scheme. We particularly used a combination of two vegetation RTM, i.e., PROSPECT [40] and SAIL [41], and a look-up-table (LUT)-based quasi-model inversion [88]. The LUT was calculated using the models in forward mode, while keeping the three parameters of interest free within reasonable parameter ranges (i.e., CAB: 10.0–70.0 $\mu g \times cm^{-2}$; CW: 0.001–0.03 $g \times cm^{-2}$; LAI: 0.1–8 $m^2 \times m^{-2}$). All other parameters were fixed to representative values (i.e., leaf structure (N): 1.8; leaf angle distribution: planophile). Applied value ranges and constants are justified by published results [37] and knowledge gathered during several field campaigns. Background optical properties (i.e., soil HCRF) were extracted from the image. The biogeophysical variable retrieval itself was based on minimizing a cost function (i.e., normalized difference between the measured and simulated HCRF signal) considering the entire wavelength range excluding the H_2O absorption features to find a LUT entry that shows the best match with a particular APEX-HCRF signature. We applied no regularization strategies at all, such as stratification of input model parameters for specific crop types, selection of most sensitive wavelength ranges, spatial constraints, or probability distribution functions of model parameters and their combinations. Canopy chlorophyll and water content were derived as products of retrieved LAI as suggested by Darvishzadeh *et al.* [89].

[1] A full list of all available attributes within SPECCHIO may be found on www.specchio.ch, comprising a total of 350 different attributes at the time of writing.

[2] The full SPECCHIO application programer interface definition can be found online: http://www.specchio.ch/doc/index.html.

IV. Case Study—Results

A. Level 1: Radiance

Radiance spectra taken by an ASD spectroradiometer were used in conjunction with calibrated white reference panel-based irradiance measurements to carry out a radiance-based validation. The MODTRAN5-based atmospheric LUT of ATCOR4 was used for the radiative transfer calculations. The entire process entails 1) inverting ground irradiance data for the best aerosol model and water vapor amount based on a RMS criterion, 2) inverting the ground irradiance below 500 nm for aerosol optical thickness, 3) using the inversion results and irradiance measurements for the radiative transfer calculation of at-sensor radiances, and 4) extracting spectra from the airborne radiance data at the location of ground measurements using a fixed window size of 5×5 pixels to account for spatial inhomogeneities. These modeled at-sensor radiances were then compared with airborne at-sensor radiances.

The results of the radiance validation are shown in Fig. 3, comparing modeled and airborne at-sensor radiances with the standard deviations indicated by error bars. RMSE values range between 11% and 15% excluding water vapor absorption bands at 1400 and 1850 nm where both airborne and *in situ* spectroradiometers contain largely noise [90].

B. Level 1: Irradiance

The overall quality of the *in situ* spectral data was assessed by analyzing the radiance time series of the white reference panel readings over the midday time period, corrected for the reflectance of the panel. The individual measurements were fitted with a polynomial and then used to compute the radiometric uncertainty for a 1° angular error of the panel

$$L_{\text{angular error}} = \frac{L \cdot \cos(\theta \pm 1^{o})}{\cos(\theta)} \quad \text{where } \theta = \text{Solar zenith angle.} \tag{6}$$

The obtained reference panel radiances are just within the 1° angular error envelope (see Fig. 4, top), confirming that the field team was very careful in adjusting the panel with a bubble level. The radiance time series also follows the change in sun elevation, confirming that the day was clear and no major irradiance fluctuations took place. Influences of instrument sensitivity changes were removed during preprocessing [51]. Changes in measured irradiance due to spatial inhomogeneity of adjacency are assumed to be minor due to the structure of the landscape, but may be represented in the scatter of irradiance values. The uncertainty envelope also illustrates the impact of the angular adjustment of the reference panel. A 1° angular error in the solar principle plane from the true horizontal results in a mean change in radiance of $\pm 0.8\%$ for the given solar zenith angle range. The dependence of the radiometry on the sun zenith angle in combination with the angular error can be observed in the uncertainty envelope in Fig. 4 (bottom) where errors are higher in the morning/afternoon and decrease toward solar noon.

The consistency of the reference panel radiance spectral time series is a prerequisite for the quality check of the irradiance estimate provided by the atmospheric correction algorithm. The global irradiance estimate was computed by ATCOR4 for the time of the overflight and compared with the irradiance calculated from white reference panel radiances interpolated over time, multiplied by π, and spectrally convolved to APEX, based on the assumption of the white reference panel being an ideal Lambertian reflector.

The global irradiance estimate computed by ATCOR4 is compared with the irradiance calculated from white reference panel radiances in Fig. 5. The two irradiances display an RMSE of 8%, excluding water vapor absorption bands at 1400 and 1850 nm, with an increased difference toward the end of the SWIR. The impact of reference panel leveling uncertainty is a negligible component of the observed bias. Fluctuations of the at-ground irradiance due to changes in atmospheric conditions between *in situ* irradiance measurement and APEX imaging times are assumed to be within the uncertainty envelope defined by the angular error.

C. Level 2: Bottom of Atmosphere HCRF

The quality of the ATCOR4-based APEX HCRF was assessed by comparing it with the HCRF of spectral ground control points (SGCPs) measured with a field spectroradiometer. Fig. 6 illustrates the comparison on the example of a vegetation target. The relative RMSE in the spectral range of 500 to 2200 nm excluding water vapor absorption bands at 1400 and 1850 nm amounts to 19% and reaches 29% when considering the full wavelength range up to 2450 nm, still excluding the water vapor absorption bands. Higher differences appear at both ends of the APEX dataset and in the water vapor absorption regions at 1400 and 1850 nm, respectively. The atmospheric correction applies interpolations to bands where low signals or sharp absorption features occur. These regions (690–736 nm, 753–770 nm, 790–838 nm, 907–983 nm, 1100–1176 nm, 1312–1514 nm, 1772–2029 nm) are indicated in Fig. 6 and should be treated with caution when using the Level 2 data.

D. Level 3: Biogeophysical Variables

A comparison on the level of retrieved biogeophysical variables was carried out on the NDVI product using a narrow band implementation and on cCAB, cCW, and LAI products using model inversion techniques. *In situ* HCRF data were spectrally convolved to APEX bands prior to biogeophysical variable retrievals. Uncertain wavelengths, i.e., water absorption bands, were removed before model inversions. In all cases, APEX derived biogeophysical variables at selected pixels coinciding with the SGCPs were plotted versus the mean variable values at the SGCPs while their standard deviation is indicated by error bars for NDVI (See Fig. 7). The model inversion was carried out on mean values, and, hence, no error bars are provided in Fig. 8.

The NDVI derived from *in situ* and APEX data shows a good agreement with an R^2 of 0.97 (see Fig. 7). However, the linear fit displays an offset of -0.127 indicating that the obtained APEX biogeophysical variable is biased. The cause for this is likely to be the near infrared band at 800 nm, which is interpolated in the APEX HCRF dataset. Illumination effects as discussed

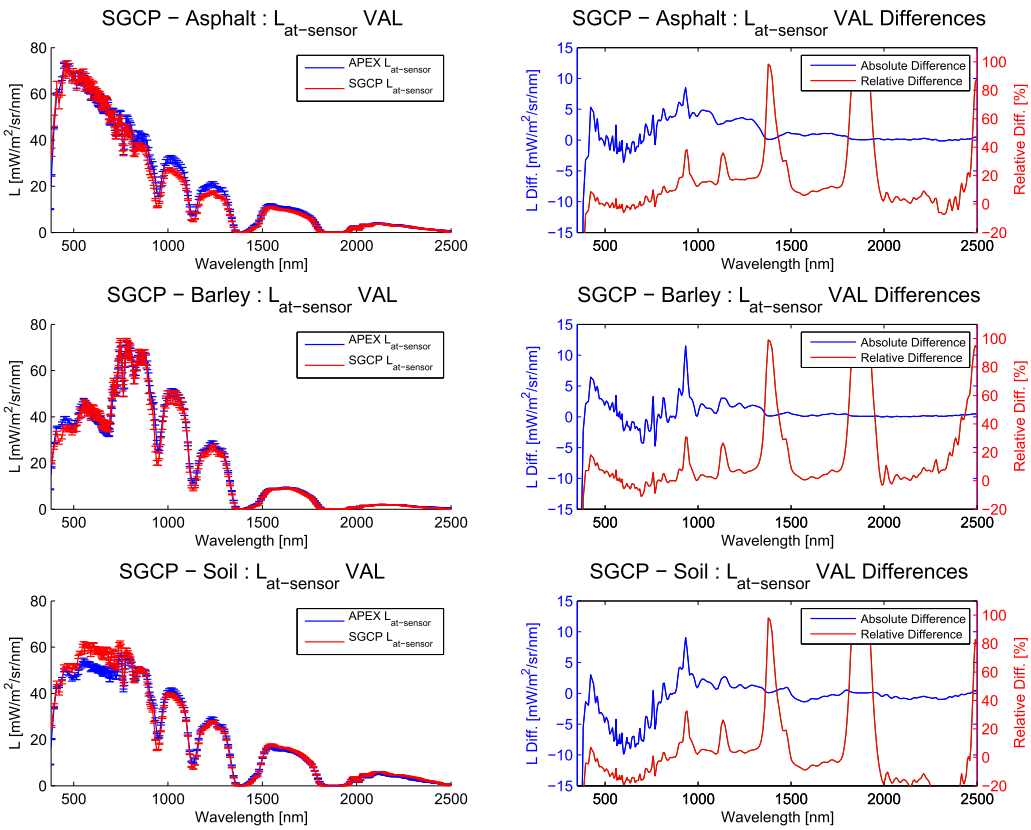

Fig. 3. Radiance (L)-based validation results of APEX imagery SGCPs for asphalt, barley, and soil at a flight altitude of 5.1 km above sea level, showing mean radiances with standard deviations indicated as error bars (left) and absolute and relative differences computed from mean spectra (right).

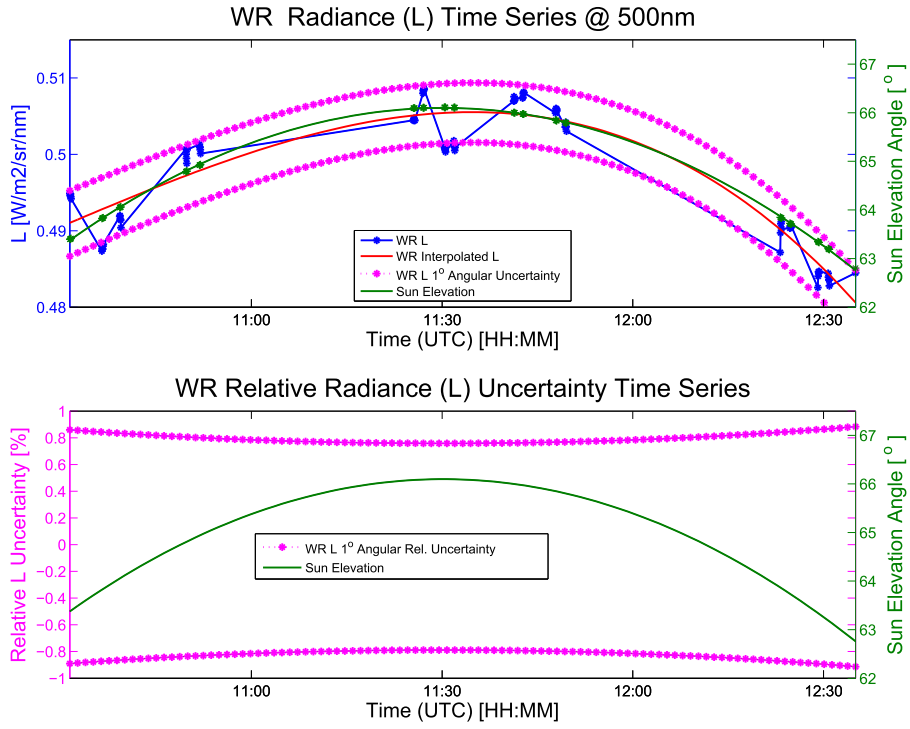

Fig. 4. Radiance of the white reference (WR) panel at 500 nm compiled over the midday period of the 17th of June field campaign, and related radiometric uncertainties due to a reference panel angular leveling error of 1° and their dependence on the sun elevation angles.

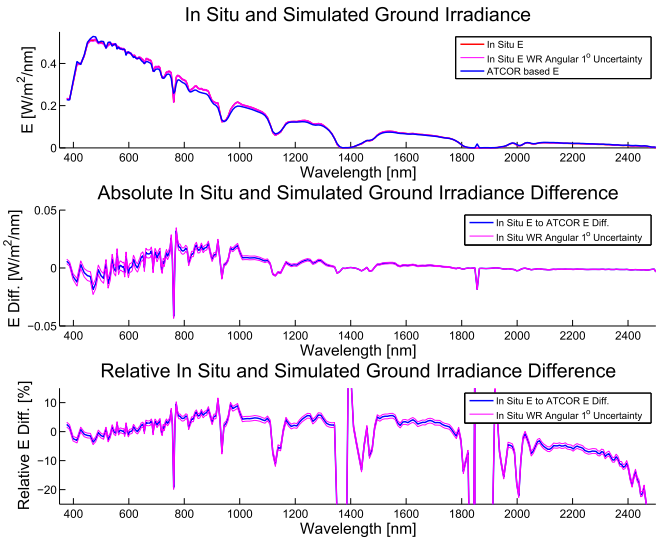

Fig. 5. Comparison of irradiance (E) simulated using ATCOR4 and computed from *in situ* white reference panel readings (top) and absolute and relative differences with indication of uncertainty due to a panel angular levelling error of 1° (middle and bottom).

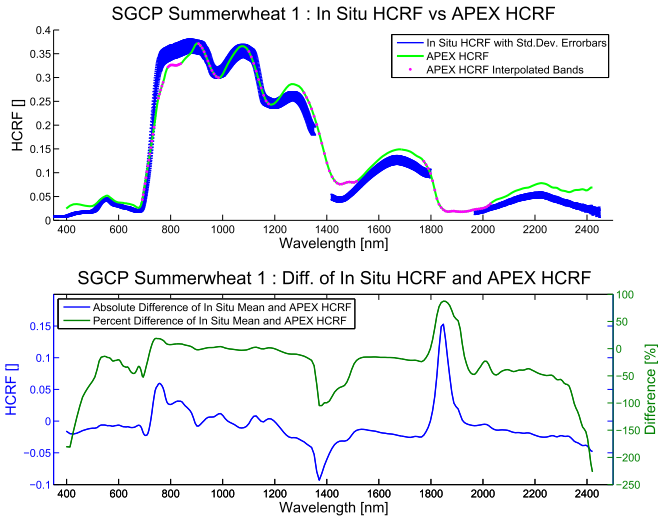

Fig. 6. Comparison of a SGCP HCRF with ATCOR4-based APEX HCRF, indicating the variability of the ground target and the interpolated bands in the ATCOR4 output (top) and the absolute and relative differences of the mean *in situ* spectrum and APEX HCRF (bottom).

in [28] can contribute to the observed bias. The relative RMSE and relative standard error of the mean are 6.7% and 6.9%, respectively. These values are rather high and mainly driven by the asphalt and soil targets, which also lead to the observed offset of the linear regression, as all vegetation targets are close to the 1:1 line.

Biochemical (cCAB and cCW) and structural (LAI) biogeophysical variables derived from *in situ* and airborne HCRF data show a moderate to good agreement with a R^2 of 0.49 for the cCAB, a R^2 of 0.63 for the cCW, and a R^2 of 0.73 for the LAI (see Fig. 8). Common to these three retrieved biogeophysical variables are deviations from the 1:1 line as well as individual biases. This reduced agreement compared to the more simple

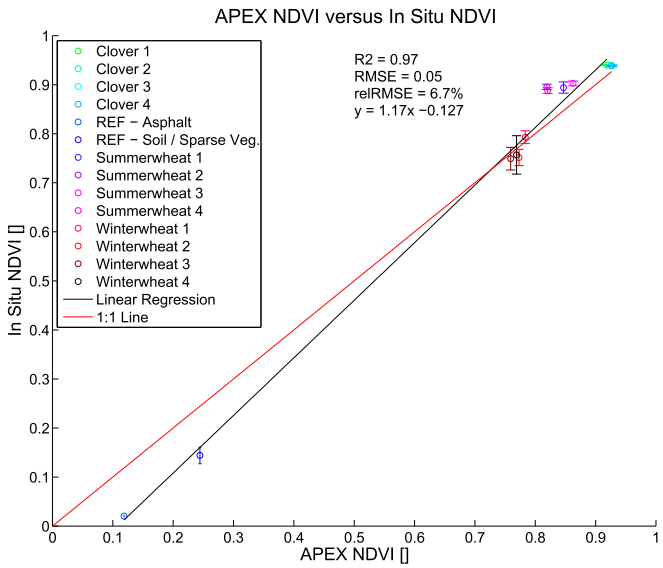

Fig. 7. Linear regression of NDVI derived from APEX and *in situ* HCRF data for different crop and surface types.

vegetation index is caused by the bulk inversion without applying any regularization. Moreover, while calculations of spectral indices have the tendency to compensate disturbing effects (i.e., illumination effects), more complex inversion schemes exploit the full information content of measured signals. Consequently, they show the divergence of information within measured HCRF if the sampling scheme of *in situ* data is not optimized for specific biogeophysical variables.

V. Discussion

A. Agreement of Physical Quantities at Field and Airborne Scale

An overarching premise of this study is the notion that there is no truth as such when it comes to data obtained by measurements, be it on ground or from remote sensing platforms. The various sources of error and uncertainty of *in situ* spectroscopy render the acquisition of accurate spectral ground data a stringent and difficult task. Table II summarizes typical agreements between *in situ* and airborne-based data products as established in this study.

The radiance level validation generally confirmed the radiometric calibration for all targets, but the nonvegetation SGCPs showed higher biases in the 600–700-nm region than the vegetation. These target-dependent biases are likely the result of a suboptimal target state for the soil SGCP where some sparse vegetation was apparent, as well as the rather small spatial size of the asphalt target where the APEX spatial point spread function may have easily covered adjacent natural targets, leading to a mixed spectral signature. The at-sensor radiance modeling utilizes the field spectrometer-based reflectance factors to simulate at-sensor radiance, and, therefore, biases in the field spectra are propagated. Simulation of the adjacency is a further source of uncertainty. Hence, it appears that the validation for spectra close to the image data average (here: vegetation types)

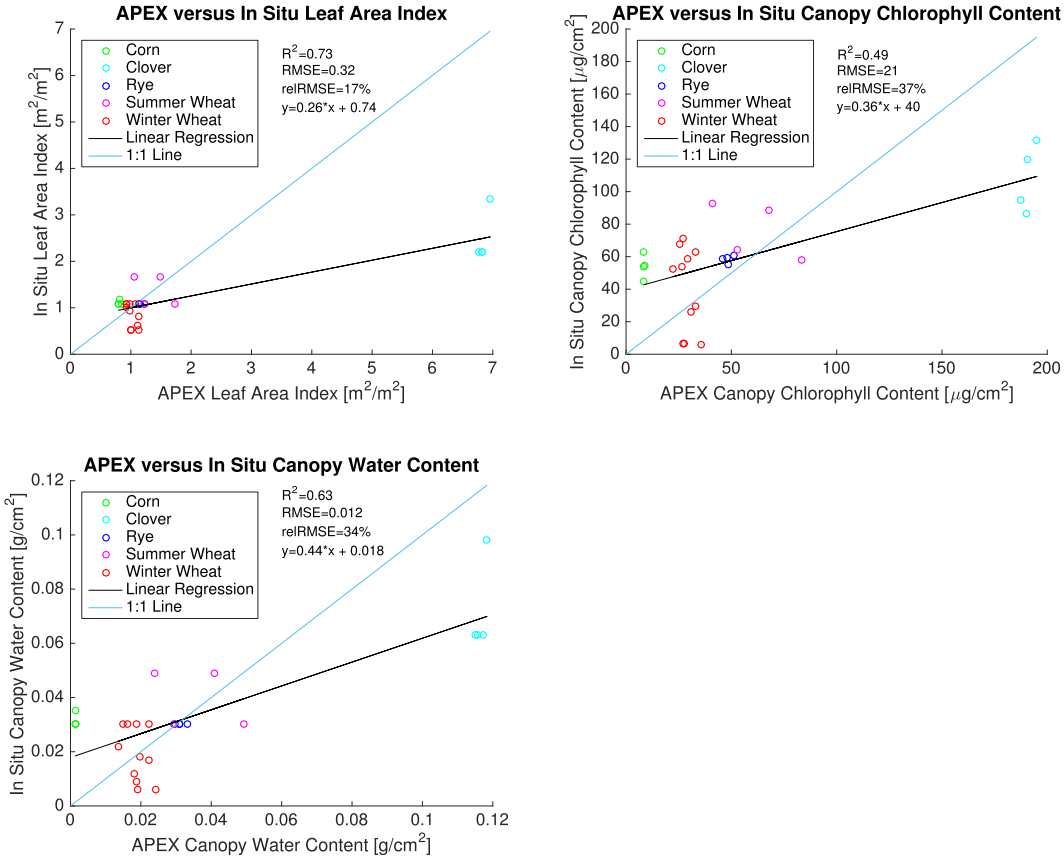

Fig. 8. Linear regression of LAI (top left), cCAB (top right), and cCW (bottom left) derived from APEX and *in situ* HCRF data for different crop types.

TABLE II
AGREEMENT OF *In Situ* AND AIRBORNE-BASED DATA PRODUCTS ACROSS PROCESSING LEVELS INDICATED BY RELATIVE ROOT-MEAN-SQUARE ERRORS AND RELATIVE STANDARD DEVIATIONS AS ESTABLISHED WITHIN THIS STUDY

Processing Level	Data Product	Rel. RMSE	Rel. Std. Deviation	Major effects limiting comparability
Level 1	Radiance	11%	6.8%	Surface heterogeneity in combination with varying spatial point spread functions and beam geometries; convolution artefacts; atmospheric characterization; white reference panel degradation
Level 1	Irradiance	8%	7.9%	Atmospheric characterization; white reference panel degradation
Level 2	HCRF	18.7%	20.6%	Above factors plus illumination effects
Level 3	Vegetation index	6.7%	6.9%	Above factors plus varying spectral point spread functions
	Plant traits	28.5%	74.7%	

performs better, whereas results are less reliable for isolated objects like bright bare soil or asphalt.

The reflectance level validation showed some differences in particular in spectral regions where APEX bands were interpolated as shown in Fig. 6. Interpolated values may differ from *in situ* values either due to radiometric miscalibrations at the edges of the interpolated regions or due to erroneous irradiance estimations.

Differences in the noninterpolated parts of the spectrum can have a variety of causes, such as wrong estimates of atmospheric composition and subsequent biases of irradiance, or radiometric miscalibrations of the airborne sensor due to incomplete sensor models or suboptimal laboratory setups (e.g., integrating sphere and optical filter interreflections that modify the radiance at the sphere port). The typical radiometric problem regions of imaging spectrometers are the UV and the blue wavelengths, as well as the end of the SWIR channel where signals are low, not only under in-flight conditions but also in laboratory settings and their correct calibration and characterization remains challenging. In this study, the APEX HCRF of the bands between 840 and 890 nm is typically underestimated and the interpolation of the red edge and the 820-nm H_2O feature is consequently biased. Reasons for this are likely to be radiometric miscalibrations of the APEX sensor due to temperature and pressure effects, currently under investigation in the framework of the European Metrology Research Program MetEOC2 project [91].

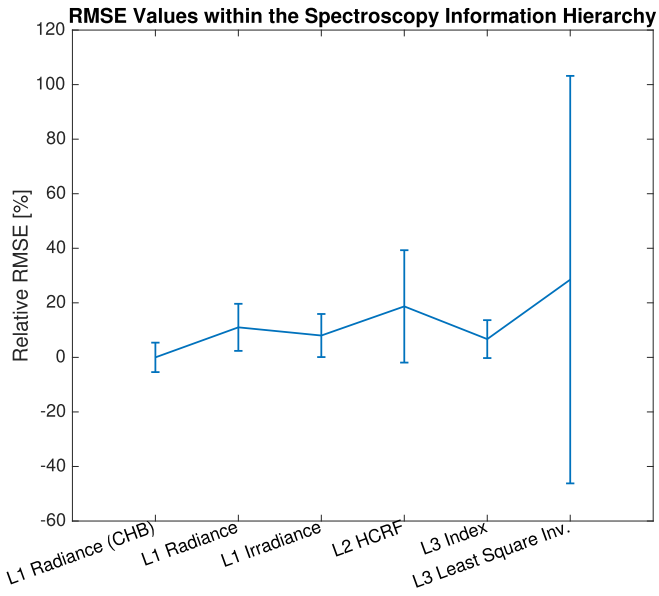

Fig. 9. Agreement of *in situ*/modeled and airborne-based data products within the spectroscopy information hierarchy stating the relative RMSE and the relative standard deviation of the errors. CHB-based uncertainty for Level 1 is derived from Schaepman *et al.* [103] and provided for completeness. Observational errors for Level 1 Radiance/Irradiance, Level 2 HCRF, Level 3 Index, and Level 3 least square inversions are based on this case study.

Observational approaches are always faced with the heterogeneity of surfaces. Table II and Fig. 9 indicate a decreasing agreement between *in situ* and airborne-based data products with increasing processing level. This effect is not only caused by the uncertain model parameterisation (e.g., of the atmosphere), but also governed by the nature of the model describing the relationship between input and output. At-sensor radiances are generally linearly related to the DNs recorded by the sensor, while e.g., a product such as chlorophyll content is subject to a nonlinear function describing the relationship between chlorophyll concentration and reflectance [92]. Consequently, errors tend to grow as small errors in the HCRF product translate into bigger biases in the computed higher level product. Vegetation indices, essentially being derived from combinations of individual spectral bands, relate more directly to HCRF data and typically show a higher agreement between *in situ* and airborne-based products compared to plant traits retrieved using complex analytical frameworks. This effect is also caused by the suppression of target brightness differences by normalising indices such as NDVI. Fig. 9 illustrates the generally bigger biases with increasing information level, with a notable drop in relative RMSE and a decreased standard error for the NDVI (Level 3 index).

The most fundamental effect compromising a direct comparison of *in situ* and airborne data is surface heterogeneity in combination with differing beam geometries and intrinsic sampling schemes (spatial point spread functions). *In situ* data are acquired in a hemispherical-conical configuration where airborne data are virtually similar with the hemispherical-directional case: field spectrometer FOVs typically range around 20° unless special fore optics are used, while, e.g., APEX has an iFOV of 0.028° [56]. The angular sensitivity of radiance measurements and subsequently derived surface information is well known [93]–[95] and is basically a combined effect of changing fractions of E^{dir} and E^{dif} and reflectance anisotropy. Damm *et al.* [28] demonstrate the large angular dependence of radiance measurements and vegetation variables retrieved from spectroscopic measurements. This sensitivity in combination with differing iFOV's (measured radiances are an integral observation over a certain angular range) can cause strong sensitivities in measured radiance signals and retrieved biogeophysical variables. Furthermore, airborne data are affected by adjacency effects, which increase with flight altitude. The detailed correction of these effects for validation purposes is to be further investigated.

Difficulties related to the estimation of surface E are an intrinsic problem of commonly used reflectance-based approaches, i.e., estimates of surface irradiance are often less representative for the underlying radiance measurement, adding uncertainty to subsequently derived HCRF data, and biogeophysical variables. It is suggested to emphasize the use of alternative retrieval schemes such as the at-sensor radiance approach (cf., [28], [37], [38]) in order to minimize the number of assumptions as applied in current processing schemes. This consequently improves the comparability of spectroscopic measurements, derived HCRF data, and retrieved biogeophysical variables across observational scales.

1) Level 1—Radiance: In spectroradiometry, the only measurable quantity is the radiant flux—there is no physical method to measure reflectance quantities other than going through radiant quantities, i.e., radiances or irradiances or the radiant flux directly. Thus, the validation on radiance level remains an indispensable task for sensor system validation, whereas validation on higher levels of processing is of high importance for data end-user quality reporting.

Accurate spectroradiometric calibrations of field and airborne spectrometers are difficult to achieve even under laboratory conditions [10], and all instruments will invariably change their properties to some degree when leaving controlled calibration environments and being exposed to various pressure and temperature regimes [59], [96]. Therefore, regular laboratory-based calibrations to reestablish traceability in combination with detailed instrument characterizations to build sensor models explaining changes of the nominal behavior are an indispensable requirement of precise radiometric measurements [5]. Such sensor models and related correction procedures are in most cases not available from the manufacturers but are established by researchers noting biases in their measurements [5], [16], [51], [59]. Consequently, end users acquiring new instrumentation are advised to carry out a thorough literature review to get to know the peculiarities of their systems before embarking on any measurement campaign [97].

2) Level 1—Irradiance: Absolute reflectance factors are only obtainable from *in situ*-based spectrometer target measurements if the irradiance field can be reliably measured. Irradiance fields with their individual diffuse and direct E components are typically measured in field spectroscopy using almost 100% reflective reference panels placed above the target, assuming a horizontally oriented and fully illuminated surface.

However, surface inclination and surface structure violate this assumption: E^{dir} can be considered as a function of the cosine of the illumination angle, while the anisotropic E^{dif} component is a function of illumination angle, atmospheric transmittance, aerosol scattering, and the adjacency effects [98]. For vegetation, the canopy structure determines changing fractions of shaded and sunlit canopy elements and geometric-optical scattering, both impacting the underlying radiative transfer. These illumination effects add an intrinsic disagreement between true and approximated surface E for any field spectroscopic measurement, and, consequently, retrieved surface HCRF and biogeophysical variables become uncertain [28]. To be more explicit on the latter point, one may consider the microstructure of a crop canopy: radiation reflected by shaded leaves contributes to the signal, but their illumination is supposed to be 100% due to the assumption of the reference panel-based reflectance estimation that equivalent amounts of irradiance reached each scene element. Consequently, the reflectance of nonhorizontal or not fully illuminated scene elements is wrongly estimated.

There are, however, also a few practical issues that lead to errors even when not considering the discussed irradiance field approximation. The involved problems include the alignment of the reference panel in 3-D space, contaminations of the panel that change its reflective properties, and spectral contamination of the panel signal by neighboring objects due to wrong pointing of the sensor.

In our case study, we have demonstrated the impact of a 1° angular error in panel alignment. From our data, it would seem reasonable to expect that angular deviations from the true horizontal of less than 1° are achievable when using a tripod and a bubble level. The errors caused by balancing the panel on the palm of the hand instead of using a tripod have been investigated during an OPTIMISE COST action summer school and indicate radiometric biases between 5% and 10%.

The contamination and degradation of reference panels additionally alters the representativeness of *in situ* irradiance measurements. Degradation of the reference panels over time is a major source of error that can be mitigated by frequent monitoring of the panel reflectance versus a laboratory standard. Typical losses in reflectance appear in the UV-Blue wavelength region just by ageing processes [99]. Fig. 10 shows a typical ageing effect where a field panel after being used for several years was compared with a pristine freshly calibrated panel under field conditions. Changes are -5% to -23% for wavelengths below 550 nm and these errors would be propagated into the measured reflectance spectra and further into derived biogeophysical variables if not compensated for.

Contamination of the reference panel radiances with neighboring target signatures due to incorrect pointing of the sensor head can as well be detected if the irradiance is assumed to be constant. In the ideal case, dividing the averages of the before-target and after-target panel radiances should result in a factor of 1 (see Fig. 11 (top)) and standard deviations of the two panel radiance sets should be similar. Any significant deviation can then be attributed to a spectral contamination (see Fig. 11 (bottom)). The shape of the negative relative standard deviation (coefficient of variation) may give indications as to what further

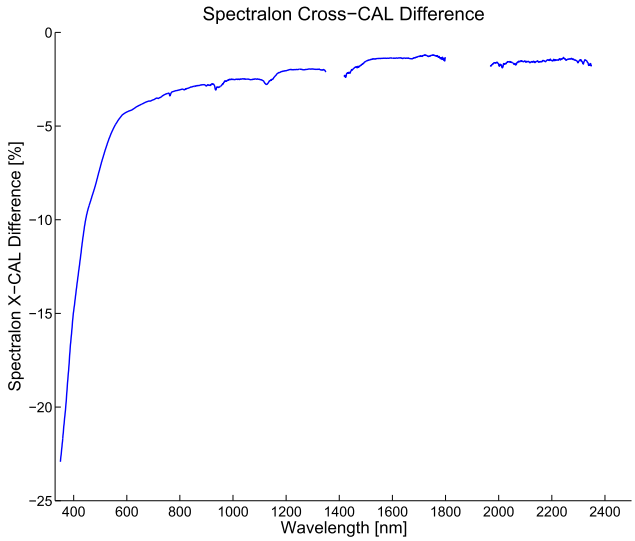

Fig. 10. Example of reference panel degradation when cross calibrated with a new pristine panel under field conditions.

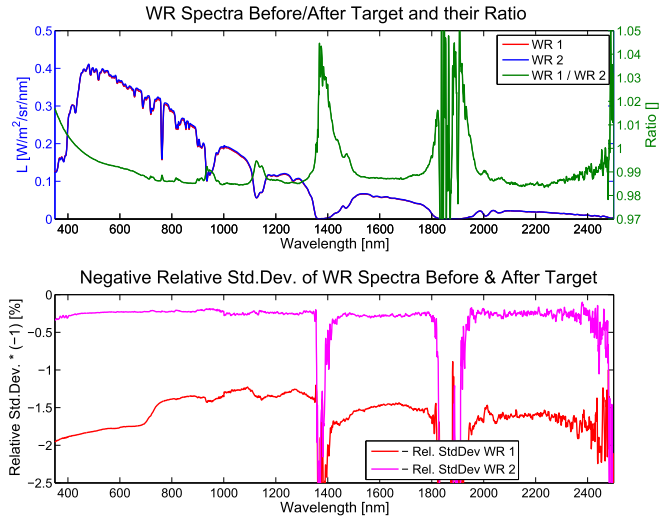

Fig. 11. Example of a white reference (WR) panel signature contamination showing visually almost identical WR panel spectra before and after target acquisition and their ratio (top) and the negative relative standard deviations with a contamination by vegetation apparent for the WR 1 acquisition (bottom).

material was present in the measurement support apart from the reference panel. In our example, the negative standard deviation resembles a vegetation spectrum. This is an interesting finding, but it has not yet been analyzed in depth and, while indicative, we feel that more research is required to develop it into a robust quality indicator.

An alternative approach, circumventing panel contamination due to dirt and neighboring scene elements by incorrect sensor pointing, would be to use calibrated irradiance measurements for reflectance retrieval as a reference rather than relying on indirect measurements of reflectance factors using a white reference panel [2].

For the airborne case, irradiance is modeled using atmospheric RTM assuming homogeneous and fully illuminated surfaces. This approach, thus, basically adds the same uncertainties due to the irradiance field approximation as described above,

but is further complicated by the need to accurately describe the status of the atmosphere. Imaging spectrometer data can themselves be used to estimate some atmospheric parameters, but these are not independent measurements, and, hence, influenced by the spectral and radiometric calibration uncertainty of the instrument. All these aspects limit the capability to compare field and airborne spectroscopy data.

3) Level 2—Reflectance Factors: The aspects that determine the agreement between *in situ* and airborne measurements, as discussed for radiance and irradiance data, also govern reflectance factor values. This makes the comparison of HCRF data from *in situ* and airborne observations most uncertain across the various processing levels (cf., Table II). A validation of airborne data using *in situ* data should only be undertaken if the SGCPs were collected with great care and if a potential violation of assumptions applied throughout the entire processing cascade is expected to be negligible.

4) Level 3—Biogeophysical Variables: Biogeophysical variables obtained from simultaneously acquired *in situ* and airborne spectroscopy data should be ultimately the same, proofing that measurements are the same as well. The above discussion outlines a wealth of different factors impacting the agreement of *in situ* and airborne spectroscopy data even if taken with care and processed with the best knowledge available. The main reason of disagreements between biogeophysical variables obtained with both measurement approaches is related to the spatial heterogeneity of surfaces and the individual and diverging spatiotemporal length scales of biogeophysical variables that can be present in a certain area. Physics of photon-surface interactions determine fluxes measurable by instruments. Therefore, slight differences in observational geometry, timing, and instrumental properties impact the information content of measured radiances and eventually also of retrieved biogeophysical variables. It is, thus, unprofessional to talk about "*ground truth*" when referring to biogeophysical variables derived from *in situ* spectral measurements. Consequently, the comparison of biogeophysical variables obtained in such manner, be it either from *in situ* or airborne data, is essentially limited. Ideally, a validation of biogeophysical variables should include their measurement via independent methods such as chemical analysis.

The aspect of instrument calibration uncertainty on derived products has recently been studied by Bachmann *et al.* [100] for the case of the EnMAP sensor. Their Monte–Carlo-based uncertainty propagation through ATCOR4 showed target-dependent NDVI uncertainties in the range of 8.2%–8.9%. This corroborates that the product errors indicated by our case study are in a reasonable range. It furthermore illustrates an example of uncertainty propagation, which should be applied to the full-processing chain.

B. Prerequisites for Quality Assessments

The extent to which *in situ* spectroscopy data quality can be evaluated depends largely on the measurement strategies and protocols, essentially defining the available information for quality assessments. Utilizing radiometrically calibrated instruments is the preferred solution as they deliver more information for quality assessments [1]. The quality check of the irradiance is one of the foremost issues as the HCRF computation assumes a constant illumination condition during the target measurement. The required data are at best acquired with a dual FOV instrument, removing the need for assumptions on the irradiance stability [2]. In the more common case of single FOV instruments, it is advisable to acquire several radiance spectra over the reference panel before and after the target acquisition. These data allow checking the stability of the irradiance by computing first- and second-order statistics for before-target and after-target panel radiance sets.

C. Metadata and Contextual Awareness

Reliable and shareable data require a strict control and documentation of the above sampling setups and environmental influences, and according metadata data should find its way into spectral data collections [5], [101] to allow automated quality indicator generation [54]. Such metadata should be sufficient to enable the contextual awareness, i.e., a full understanding of the circumstances of data acquisition. Modern spectral information systems are essentially capable of storing unlimited numbers of metaparameters [61], [62]. However, entering these data in a consistent [54] and timely manner while field records are still available and personal recollections yet fresh is definitely problematic. As a matter of fact, the metadata of this study were only properly compiled within SPECCHIO for the purpose of providing consistent analysis for this very paper. We have found this experience a rather frustrating one as it was exceedingly time consuming, starting with fundamental issues such as the time zone of the acquisition time stamps. In some cases, no satisfying reason could be found as to why a certain SGCP was radiometrically biased. Consequently, the perpetual first level of quality starts with the education and training of field personnel, impressing on them the importance of strict adherence to field protocols and thorough documentation to support the identification of error sources later on. Similarly vital is an understanding of the physics involved in the light and matter interactions. In particular, the biases caused by panel angular alignment errors are often not recognized, and the effective irradiance given by the illumination zenith angle relative to the panel surface is confounded with the Lambertian property that results theoretically in an angular independence of reflected radiance on the viewing angle.

Modern technology such as inclinometers and automated systems may be used to take the human errors out of the equation and log metadata describing the sampling procedure and environment. This leaves the complexities of the measurement protocol to be applied [5], [101], which must deal with time and space in a way relevant to the scientific question to be answered and the process to be investigated. Either way, the meticulous collection of metadata and spectral data, the latter ideally as radiance, is the key to developing quantitative quality indicators during postprocessing and to finding explanations for irregularities.

D. Reliability and Representativeness of this Case Study

Cross-validation exercises should be approached with care, keeping in mind that all measurement results are inherently

uncertain. *In situ* data may be used to constrain the biases of airborne- and space-based data and vice versa, utilizing data at various processing levels to implement as many quality checks as possible within the processing chain. Data storage and processing infrastructures that handle spectroscopy data and metadata in a repeatable manner are, thus, a key component for the consistent generation of cross-validated data products within the spectroscopy information hierarchy. Restrictions to this are caused by measurement setup differences (observation geometry, FOV, and spatial scales and representativeness), operator errors, unsuitable protocols for the application in question, uncertainties due to limited control over the equipment position in time and space, and inherent uncertainties caused by assumptions of the representativeness of reference panel measurements.

Thus, while greatest care has been taken in preparing and analyzing the dataset used in this case study, it still includes some biases in both *in situ* data and airborne that could not yet be properly identified. The general areas requiring particular attention are 1) representativeness of SGCPs due to spatial inhomogeneities, measurement errors, and missing metadata for postinterpretation, 2) detailed airborne sensor models to compensate for environmental conditions like pressure and temperature, and 3) parameterization of RTM to replicate the irradiance and scattering conditions during image acquisition.

The error budgets stated in this study are based on a few data points only and should be taken as indications rather than established figures. The stated uncertainties are based on the standard deviation of the differences between airborne and *in situ* based data, i.e., the standard error, and are not to be mistaken as propagated uncertainties.

The time, software, and expertize required to carry out all cross-validations outlined in this study may be well beyond the resources and capabilities of a typical imaging spectroscopy end user. This realization strongly advocates a better cross-validation methodology support via specialized software written to this extent. Furthermore, a propagated uncertainty estimate, throughout the spectroscopy acquisition and processing stages, i.e., traceability [91], [102], should be embraced by the community and implemented in the relevant software packages.

VI. Conclusion

This study collates methods and recommended practices of field spectroscopy accumulated within the research community over the past decades and presents validation techniques in support of field and airborne spectroscopy. Experienced spectroscopy scientists should find the work insofar interesting as that complications of instruments, software, fieldwork, protocols, calibration, characterization, and traceability, already treated two decades ago, are still relevant today and reliable spectroscopy is still no off-the-shelf product. Researchers new to the field will find references herein to relevant work and findings established in the past, compiled in a succinct manner to quickly establish an overview of the complexities of field spectroscopy.

The sources of error within airborne and *in situ* sensor-based data are manifold and a comparison between such datasets is further complicated by scale dependencies and differing observational geometries. If one thing may be gleaned from the presented case study, it is the realization that a lack of metadata severely limits the interpretation of results, simply because the exact nature of the measurement process and the environmental conditions at the time of data acquisition are unclear and cannot be precisely replicated. Hence, the attribution of the cause of observed differences is wrought with difficulties and often remains speculative. The RMSE and related standard deviations reported for the presented case study may be taken as indicative of the errors one may expect and should prompt users to carry out their own error assessment for their individual datasets.

The key to advances in field and airborne spectroscopy is fourfold and encompasses 1) the development of smarter instruments gathering relevant metadata in an automated fashion, 2) the detailed study of irradiance fields within the iFOV of spectroradiometers, 3) the design of spectral processing and storage software that can handle spectral data and their metadata including the propagation of uncertainty, and 4) last but not least the education of the spectroscopy researchers to foster the understanding of interactions between light and matter and the implications of measuring these phenomena using spectroradiometric systems.

References

[1] E. J. Milton, M. E. Schaepman, K. Anderson, M. Kneubühler, and N. Fox, "Progress in field spectroscopy," *Remote Sens. Environ.*, vol. 113, Suppl. 1, pp. S92–S109, 2009.

[2] A. Mac Arthur and I. Robinson, "A critique of field spectroscopy and the challenges and opportunities it presents for remote sensing for agriculture, ecosystems, and hydrology," *Proc. SPIE*, vol. 9637, pp. 1–11, 2015.

[3] E. C. Barett and L. F. Curtis, *Introduction to Environmental Remote Sensing*, 3rd ed. New York, NY, USA: Springer, 2009.

[4] GEO and CEOS, "A quality assurance framework for earth observation: Operational guidelines," *Group Earth Observations/Committee Earth Observation Satellites*, 2008.

[5] T. H. Hemmer and T. L. Westphal, "Lessons learned in the post-processing of field spectroradiometric data covering the 0.4 to 2.5 μm wavelength region," *Proc. SPIE* 4049, Algorithms for Multispectral, Hyperspectral, and Ultraspectral Imagery VI, pp 249–260. (August 23, 2000) doi: 10.1117/12.410347.

[6] G. P. Petropoulos, K. Manevski, and T. N. Carlson, "Hyperspectral remote sensing with emphasis on land cover mapping: From ground to satellite observations," in *Scale Issues in Remote Sensing*. New York, NY, USA: Wiley, 2014, pp. 285–320.

[7] F. Zhao *et al.*, "Simulated impact of sensor field of view and distance on field measurements of bidirectional reflectance factors for row crops," *Remote Sens. Environ.*, vol. 156, pp. 129–142, 2015.

[8] L. Pompilio, P. Villa, M. Boschetti, and M. Pepe, "Spectroradiometric field surveys in remote sensing practice: A workflow proposal, from planning to analysis," *IEEE Geosci. Remote Sens. Mag.*, vol. 1, no. 2, pp. 37–51, Jun. 2013.

[9] M. E. Schaepman and S. Dangel, "Solid laboratory calibration of a nonimaging spectroradiometer," *Appl. Opt.*, vol. 39, pp. 3754–3764, Jul. 7, 2000.

[10] H. Kostkowski, *Reliable Spectroradiometry*. La Plata, MA, USA: Spectroradiometry Consulting, 1997.

[11] K. Anderson and E. J. Milton, "On the temporal stability of ground calibration targets: Implications for the reproducibility of remote sensing methodologies," *Int. J. Remote Sens.*, vol. 27, pp. 3365–3374, 2006.

[12] K. Anderson *et al.*, "Inter-comparison of hemispherical conical reflectance factors (HCRF) measured with four fibre-based spectrometers," *Opt. Exp.*, vol. 21, pp. 605–617, Jan. 14, 2013.

[13] M. Balzarolo *et al.*, "Ground-based optical measurements at european flux sites: A review of methods, instruments and current controversies," *Sensors*, vol. 11, pp. 7954–7981, 2011.

[14] K. Anderson, J. L. Dungan, and A. MacArthur, "On the reproducibility of field-measured reflectance factors in the context of vegetation studies," *Remote Sens. Environ.*, vol. 115, pp. 1893–1905, 2011.

[15] G. Schaepman-Strub, M. Schaepman, T. H. Painter, S. Dangel, and J. V. Martonchik, "Reflectance quantities in optical remote sensing—Definitions and case studies," *Remote Sens. Environ.*, vol. 103, pp. 27–42, 2006.

[16] J. Pacheco-Labrador and M. Martín, "Characterization of a field spectroradiometer for unattended vegetation monitoring. Key sensor models and impacts on reflectance," *Sensors*, vol. 15, pp. 4154–4175, 2015.

[17] A. Damm *et al.*, "Modeling the impact of spectral sensor configurations on the FLD retrieval accuracy of sun-induced chlorophyll fluorescence," *Remote Sens. Environ.*, vol. 115, pp. 1882–1892, 2011.

[18] K. T. Kriebel, "On the variability of the reflected radiation field due to differing distributions of the irradiation," *Remote Sens Environ.*, vol. 4, pp. 257–264, 1976.

[19] K. T. Kriebel, "Average variability of the radiation reflected by vegetated surfaces due to differing irradiations," *Remote Sens. Environ.*, vol. 7, pp. 81–83, 1978.

[20] K. T. Kriebel, "Albedo of vegetated surfaces: Its variability with differing irradiances," *Remote Sens. Environ.*, vol. 8, pp. 283–290, 1979.

[21] C. S. T. Daughtry, V. C. Vanderbilt, and V. J. Pollara, "Variability of reflectance measurements with sensor altitude and canopy type," *Agronomy J.*, vol. 74, pp. 744–751, 1982.

[22] A. MacArthur, C. J. MacLellan, and T. Malthus, "The fields of view and directional response functions of two field spectroradiometers," *IEEE Trans. Geosci. Remote Sens.*, vol. 50, no. 10, pp. 3892–3907, Oct. 2012.

[23] L. Chisholm and A. Hueni, "The spectroscopy dataset lifecycle: Best practice for exchange and dissemination," in *AusCover Good Practice Guidelines: A technical Handbook Supporting Calibration and Validation Activities of Remotely Sensed Data Product*, A. Held, S. Phinn, M. Soto-Berelov, and S. D. Jones, Eds. Canberra, Australia: TERN AusCover, 2015, pp. 234–248.

[24] L. Floridi, "Is information meaningful data?," *Phil. Phenomenol. Res.*, vol. 70, pp. 351–370, 2005.

[25] J. Rowley, "The wisdom hierarchy: Representations of the DIKW hierarchy," *J. Inf. Sci.*, vol. 33, pp. 163–180, 2007.

[26] W. Verhoef, "Earth observation modeling based on layer scattering matrices," *Remote Sens. Environ.*, vol. 17, pp. 165–178, Jan. 4, 1985.

[27] W. Verhoef and H. Bach, "Coupled soil–leaf-canopy and atmosphere radiative transfer modeling to simulate hyperspectral multi-angular surface reflectance and TOA radiance data," *Remote Sens. Environ.*, vol. 109, pp. 166–182, Jul. 30, 2007.

[28] A. Damm, L. Guanter, W. Verhoef, D. Schläpfer, S. Garbari, and M. E. Schaepman, "Impact of varying irradiance on vegetation indices and chlorophyll fluorescence derived from spectroscopy data," *Remote Sens. Environ.*, vol. 156, pp. 202–215, 2015.

[29] F. E. Nicodemus, J. C. Richmond, J. J. Hsia, I. W. Ginsberg, and T. Limperis, "Geometrical considerations and nomenclature for reflectance," Institute for Basic Standards, National Bureau of Standards, Washington, DC, USA, 1977.

[30] E. J. Milton, "Review article principles of field spectroscopy," *Int. J. Remote Sens.*, vol. 8, pp. 1807–1827, 1987.

[31] G. Schaepman-Strub, M. E. Schaepman, J. V. Martonchik, S. Dangel, and T. Painter, "Terminology of radiometry and reflectance—From concepts to measured quantities," in *The SAGE Handbook of Remote Sensing*, T. A. Warner, M. D. Nellis, and G. Foody, Eds. London, U.K.: Sage, 2009, pp. 215–228.

[32] R. Casa and H. G. Jones, "Retrieval of crop canopy properties: A comparison between model inversion from hyperspectral data and image classification," *Int. J. Remote Sens.*, vol. 25, pp. 1119–1130, Jan. 3, 2004.

[33] A. Burkart, H. Aasen, L. Alonso, G. Menz, G. Bareth, and U. Rascher, "Angular dependency of hyperspectral measurements over wheat characterized by a novel UAV based goniometer," *Remote Sens.*, vol. 7, pp. 725–746, 2015.

[34] J. Verrelst, M. E. Schaepman, B. Koetz, and M. Kneubühler, "Angular sensitivity analysis of vegetation indices derived from CHRIS/PROBA data," *Remote Sens. Environ.*, vol. 112, pp. 2341–2353, 2008.

[35] S. L. Liang, "Recent developments in estimating land surface biogeophysical variables from optical remote sensing," *Prog. Phys. Geogr.*, vol. 31, pp. 501–516, Oct. 2007.

[36] Y. Knyazikhin *et al.*, "Hyperspectral remote sensing of foliar nitrogen content," *Proc. Nat. Acad. Sci. USA*, vol. 110, pp. E185–E192, Jan. 15, 2013.

[37] V. C. E. Laurent, W. Verhoef, A. Damm, M. E. Schaepman, and J. G. P. W. Clevers, "A Bayesian object-based approach for estimating vegetation biophysical and biochemical variables from APEX at-sensor radiance data," *Remote Sens. Environ.*, vol. 139, pp. 6–17, Dec. 2013.

[38] V. C. E. Laurent, W. Verhoef, J. G. P. W. Clevers, and M. E. Schaepman, "Inversion of a coupled canopy-atmosphere model using multi-angular top-of-atmosphere radiance data: A forest case study," *Remote Sens. Environ.*, vol. 115, pp. 2603–2612, 2011.

[39] M. E. Schaepman, S. L. Ustin, A. J. Plaza, T. H. Painter, J. Verrelst, and S. L. Liang, "Earth system science related imaging spectroscopy—An assessment," *Remote Sens. Environ.*, vol. 113, pp. S123–S137, Sep. 2009.

[40] S. Jacquemoud and F. Baret, "PROSPECT: A model of leaf optical properties spectra," *Remote Sens. Environ.*, vol. 34, pp. 75–91, 1990.

[41] W. Verhoef, "Light scattering by leaf layers with application to canopy reflectance modeling: The SAIL model," *Remote Sens. Environ.*, vol. 16, pp. 125–141, 1984.

[42] M. E. Schaepman, S. L. Ustin, A. J. Plaza, T. H. Painter, J. Verrelst, and S. Liang, "Earth system science related imaging spectroscopy—An assessment," *Remote Sens. Environ.*, vol. 113, pp. S123–S137, Sep. 2009.

[43] S. Garrigues, D. Allard, F. Baret, and M. Weiss, "Quantifying spatial heterogeneity at the landscape scale using variogram models," *Remote Sens. Environ.*, vol. 103, pp. 81–96, 2006.

[44] J. A. Gamon and J. A. Berry, "Facultative and constitutive pigment effects on the photochemical reflectance index (PRI) in sun and shade conifer needles," *Israel J. Plant Sci.*, vol. 60, pp. 85–95, 2012.

[45] J. G. P. W. Clevers, L. Kooistra, and M. E. Schaepman, "Estimating canopy water content using hyperspectral remote sensing data," *Int. J. Appl. Earth Obs. Geoinf.*, vol. 12, pp. 119–125, Apr. 2010.

[46] G. Rallo, M. Minacapilli, G. Ciraolo, and G. Provenzano, "Detecting crop water status in mature olive groves using vegetation spectral measurements," *Biosyst. Eng.*, vol. 128, pp. 52–68, Dec. 2014.

[47] A. F. Goetz, "Making accurate field spectral reflectance measurements," ASD Inc., Boulder, CO, USA, 2012, p. 16.

[48] C. J. Bruegge, A. E. Stiegman, D. R. Coulter, R. R. Hale, D. J. Diner, and A. W. Springsteen, "Reflectance stability analysis of Spectralon diffuse calibration panels," *Proc. SPIE*, vol. 1493, pp. 132–142, 1991.

[49] E. M. Rollin, E. J. Milton, and D. R. Emery, "Reference panel anisotropy and diffuse radiation—Some implications for field spectroscopy," *Int. J. Remote Sens.*, vol. 21, pp. 2799–2810, 2000.

[50] D. S. Kimes, J. A. Kirchner, and W. W. Newcomb, "Spectral radiance errors in remote sensing ground studies due to nearby objects," *Appl. Opt.*, vol. 22, pp. 8–10, 1983.

[51] Hueni, A. and Bialek, A., "Cause, effect and correction of field spectroradiometer inter-channel radiometric steps," *IEEE J. Sel. Topics Appl. Earth Observ. Remote Sens.*, 2016, to be published.

[52] B. Rasaiah, S. Jones, C. Bellman, and T. Malthus, "Critical metadata for spectroscopy field campaigns," *Remote Sens.*, vol. 6, pp. 3662–3680, 2014.

[53] A. Hueni, J. Nieke, J. Schopfer, M. Kneubühler, and K. I. Itten, "The spectral database SPECCHIO for improved long-term usability and data sharing," *Comput. Geosci.*, vol. 35, pp. 557–565, 2009.

[54] B. Rasaiah, S. Jones, C. Bellman, T. Malthus, and A. Hueni, "Assessing field spectroscopy metadata quality," *Remote Sens.*, vol. 7, pp. 4499–4526, 2015.

[55] SPECCHIO Spectral Information System. (2016). [Online]. Available: http://www.specchio.ch

[56] M. Schaepman *et al.*, "Advanced radiometry measurements and earth science applications with the airborne prism experiment (APEX)," *Remote Sens. Environ.*, vol. 158, pp. 207–219, 2015.

[57] A. P. Cracknell, "Review article synergy in remote sensing-what's in a pixel?," *Int. J. Remote Sens.*, vol. 19, pp. 2025–2047, Jan. 1, 1998.

[58] A. Hueni, K. Lenhard, A. Baumgartner, and M. Schaepman, "The APEX (airborne prism experiment-imaging spectrometer) calibration information system," *IEEE Trans. Geosci. Remote Sens.*, vol. 51, no. 11, pp. 5169–5180, Nov. 2013.

[59] A. Hueni, D. Schlaepfer, M. Jehle, and M. E. Schaepman, "Impacts of dichroic prism coatings on radiometry of the airborne imaging spectrometer APEX," *Appl. Opt.*, vol. 53, pp. 5344–5352, 2014.

[60] A. Hueni *et al.*, "Structure, components and interfaces of the airborne prism experiment (APEX) processing and archiving facility," *IEEE Trans. Geosci. Remote Sens.*, vol. 47, no. 1, pp. 29–43, Jan. 2009.

[61] A. Hueni, J. Nieke, J. Schopfer, M. Kneubühler, and K. Itten, "The spectral database SPECCHIO for improved long term usability and data sharing," *Comput. Geosci.*, vol. 35, pp. 557–565, 2009.

[62] A. Hueni, L. Chisholm, L. Suarez, C. Ong, and M. Wyatt, "Spectral information system development for Australia," in *Proc. Geospatial Sci. Res. Symp.*, Melbourne, Australia, 2012, pp. 1–11.

[63] D. R. Taubert *et al.*, "Providing radiometric traceability for the calibration home base of DLR by PTB," *AIP Conf. Proc.,* vol. 1531, pp. 376–379, 2013.

[64] V. R. C. E. Laurent, M. E. Schaepman, W. Verhoef, J. Weyermann, and R. O. Chavez, "Bayesian object-based estimation of LAI and chlorophyll from a simulated sentinel-2 top-of-atmosphere radiance image," *Remote Sens. Environ.*, vol. 140, pp. 318–329, 2014.

[65] K. J. Thome, "Absolute radiometric calibration of Landsat 7 ETM+ using the reflectance-based method," *Remote Sens. Environ.*, vol. 78, pp. 27–38, 2001.

[66] P. N. Slater *et al.*, "Reflectance- and radiance-based methods for the in-flight absolute calibration of multispectral sensors," *Remote Sens. Environ.*, vol. 22, pp. 11–37, Jun. 1987.

[67] K. Thome, C. L. Gustafson–Bold, P. N. Slater, and W. H. Farrand, "In–flight radiometric calibration of HYDICE using a reflectance-based approach," *Proc. SPIE*, vol. 2821, pp. 311–319, 1996.

[68] R. Richter, D. Schlaepfer, and A. Mueller, "Operational atmospheric correction for imaging spectrometers accounting for the smile effect," *IEEE Trans. Geosci. Remote Sens.*, vol. 49, no. 5, pp. 1772–1780, May 2011.

[69] R. Richter and D. Schläpfer, "Geo-atmospheric processing of airborne imaging spectrometry data. Part 2: Atmospheric/topographic correction," *Int. J. Remote Sens.*, vol. 23, pp. 2631–2649, 2002.

[70] R. Zurita-Milla, J. Clevers, M. E. Schaepman, and M. Kneubühler, "Effects of MERIS L1b radiometric calibration on regional lan cover mapping and land products," *Int. J. Remote Sens.*, vol. 28, pp. 653–673, 2007.

[71] A. Damm, L. Guanter, W. Verhoef, D. Schläpfer, S. Garbari, and M. E. Schaepman, "Impact of varying irradiance on vegetation indices and chlorophyll fluorescence derived from spectroscopy data," *Remote Sens. Environ.*, vol. 156, pp. 202–215, 2015.

[72] R. Richter and D. Schläpfer, "Atmospheric/topographic correction for airborne imagery," *DLR-IB 565-02, 7.0.0 ed, German Aerospace Center*, Wessling, Germany, 2015.

[73] J. Schopfer, S. Dangel, M. Kneubühler, and K. I. Itten, "The improved dual-view field goniometer system FIGOS," *Sensors*, vol. 8, pp. 5120–5140, 2008.

[74] S. Dangel, M. M. Verstraete, J. Schopfer, M. Kneubühler, M. Schaepman, and K. I. Itten, "Toward a direct comparison of field and laboratory goniometer measurements," *IEEE Trans. Geosci. Remote Sens.*, vol. 43, no. 11, pp. 2666–2675, Nov. 2005.

[75] M. Jehle, A. Hueni, K. Lenhard, A. Baumgartner, and M. E. Schaepman, "Detection and correction of radiance variations during spectral calibration in APEX," *IEEE Geosci. Remote Sens. Lett.*, vol. 12, no. 5, pp. 1023–1027, Dec. 2014.

[76] A. Hueni, S. Sterckx, and M. Jehle, "Operational calibration of APEX," in *Proc. IEEE Int. Geosci. Remote Sens. Symp.*, Melbourne, Vic., Australia, 2013, pp. 4423–4426.

[77] A. Hueni *et al.*, "Operational status of APEX and characteristics of the APEX open science data set," in *Proc. IEEE Int. Geosci. Remote Sens. Symp.*, Munich, Germany, 2012, pp. 5009–5012.

[78] P. Gege *et al.*, "Calibration facility for airborne imaging spectrometers," *ISPRS J. Photogramm. Remote Sens.*, vol. 64, pp. 387–397, 2009.

[79] M. Bachmann *et al.*, "Generic quality indicators and quality layers," *EUFAR FP7 JRA2-HYQUAPRO*, 2010.

[80] A. Berk *et al.*, "MODTRAN5: A reformulated atmospheric band model with auxiliary species and practical multiple scattering options," *Proc. SPIE*, vol. 5655, pp. 662–667, 2005.

[81] D. Schläpfer and R. Richter, "Geo-atmospheric processing of airborne imaging spectrometry data. Part 1: Parametric orthorectification," *Int. J. Remote Sens.*, vol. 23, pp. 2609–2630, Jul. 2002.

[82] T. D. Wason and D. Wiley, "Structured metadata spaces," *J. Internet Cataloging*, vol. 3, pp. 263–277, 2000.

[83] C. J. Tucker, "Red and photographic infrared linear combinations for monitoring vegetation," *Remote Sens. Environ.*, vol. 8, pp. 127–150, 1979.

[84] J. W. J. Rouse, R. H. Haas, J. A. Schell, and D. W. Deering, "Monitoring vegetation systems in the great plains with ERTS," in *Proc. 3rd Earth Resour. Technol. Satellite Symp.*, 1973, pp. 309–317.

[85] D. Haboudane, J. R. Miller, E. Pattey, P. J. Zarco-Tejada, and I. B. Strachan, "Hyperspectral vegetation indices and novel algorithms for predicting green LAI of crop canopies: Modeling and validation in the context of precision agriculture," *Remote Sens. Environ.*, vol. 90, pp. 337–352, 2004.

[86] S. Jacquemoud *et al.*, "PROSPECT + SAIL models: A review of use for vegetation characterization," *Remote Sens. Environ.*, vol. 113, pp. S56–S66, 2009.

[87] V. C. E. Laurent, M. E. Schaepman, W. Verhoef, J. Weyermann, and R. O. Chavez, "Bayesian object-based estimation of LAI and chlorophyll from a simulated sentinel-2 top-of-atmosphere radiance image," *Remote Sens. Environ.*, vol. 140, pp. 318–329, Jan. 2014.

[88] B. Combal *et al.*, "Retrieval of canopy biophysical variables from bidirectional reflectance using prior information to solve the ill-posed inverse problem," *Remote Sens. Environ.*, vol. 84, pp. 1–15, 2003.

[89] R. Darvishzadeh, A. Skidmore, M. Schlerf, and C. Atzberger, "Inversion of a radiative transfer model for estimating vegetation LAI and chlorophyll in a heterogeneous grassland," *Remote Sens. Environ.*, vol. 112, pp. 2592–2604, May 2008.

[90] J. Secker, K. Staenz, R. P. Gauthier, and P. Budkewitsch, "Vicarious calibration of airborne hyperspectral sensors in operational environments," *Remote Sens. Environ.*, vol. 76, pp. 81–92, 2001.

[91] Metrology for Earth Observation and Climate. (2016). [Online]. Available: http://www.emceoc.org

[92] C. V. Barton, "A theoretical analysis of the influence of heterogeneity in chlorophyll distribution on leaf reflectance," *Tree Physiol.*, vol. 21, pp. 789–795, 2001.

[93] C. V. M. Barton and P. R. J. North, "Remote sensing of canopy light use efficiency using the photochemical reflectance index—Model and sensitivity analysis," *Remote Sens. Environ.*, vol. 78, pp. 264–273, Dec. 2001.

[94] J. Weyermann, A. Damm, M. Kneubuhler, and M. E. Schaepman, "Correction of reflectance anisotropy effects of vegetation on airborne spectroscopy data and derived products," *IEEE Trans. Geosci. Remote Sens.*, vol. 52, no. 1, pp. 616–627, Jan. 2014.

[95] G. Feng, J. Yufang, C. B. Schaaf, and A. H. Strahler, "Bidirectional NDVI and atmospherically resistant BRDF inversion for vegetation canopy," *IEEE Trans. Geosci. Remote Sens.*, vol. 40, no. 6, pp. 1269–1278, Jun. 2002.

[96] N. Fox *et al.*, "Traceable radiometry underpinning terrestrial- and heliostudies (TRUTHS)," *Adv. Space Res.*, vol. 32, pp. 2253–2261, 2003.

[97] J. C. Wallis *et al.*, "Know thy sensor: Trust, data quality, and data integrity in scientific digital libraries," in *Lecture Notes in Computer. Science*, vol. 4675. Berlin, Germany: Springer, 2007, pp. 380–391.

[98] J. E. Hay, "Calculation of monthly mean solar radiation for horizontal and inclined surfaces," *Sol. Energy*, vol. 23, pp. 301–307, 1979.

[99] W Möller, K. P Nikolaus, and A. Höpe, "Degradation of the diffuse reflectance of spectralon under low-level irradiation," *Metrologia*, vol. 40, pp. 212–215, 2003.

[100] M. Bachmann, A. Makarau, K. Segl, and R. Richter, "Estimating the influence of spectral and radiometric calibration uncertainties on EnMAP data products—Examples for ground reflectance retrieval and vegetation indices," *Remote Sens.*, vol. 7, pp. 10689–10714, 2015.

[101] K. Pfitzner, A. Bollhöfer, and G. Carr, "A standard design for collecting vegetation reference spectra: Implementation and implications for data sharing," *J. Spatial Sci.*, vol. 51, pp. 79–92, 2006.

[102] N. Fox *et al.*, "Accurate radiometry from space: An essential tool for climate studies," *Philosoph. Trans. Roy. Soc. A, Math., Phys. Eng. Sci.*, vol. 369, pp. 4028–4063, 2011.

[103] M. E. Schaepman *et al.*, "Advanced radiometry measurements and earth science applications with the airborne prism experiment (APEX)," *Remote Sens. Environ.*, vol. 158, pp. 207–219, 2015.

Andreas Hueni (M'12) received the B.Sc. degree in computer science from the University of Applied Science Brugg-Windisch, Brugg, Switzerland, in 1997, the PGDip degree in geographic information systems and M.Phil. (Sc.) degree in earth science from Massey University, Palmerston North, New Zealand, in 2005 and 2006, respectively, and the Ph.D. degree in geography from the University of Zurich (UZH), Zurich, Switzerland, in 2011.

He has been working in the APEX Project since 2007 and is currently a Research Associate with the Remote Sensing Laboratories, UZH, responsible for APEX sensor and data calibration. His research interests include calibration of spectrometers and the design of combined database and software systems such as the spectral database SPECCHIO.

Alexander Damm received the Diploma (M.Sc.) degree and the Ph.D. (Dr.rer.Nat.) degree in geography from the Humboldt University, Berlin, Germany, in 2004 and 2008, respectively.

He is currently a Lecturer with the Remote Sensing Laboratories, University of Zurich, Zurich, Switzerland, and leading a research group studying processes of vegetation ecosystems in response to dynamic environmental conditions. He is a responsible Project Manager with the Swiss Earth Observatory Network, a competence center to monitor status and functioning of ecosystems using combined observational-modeling approaches. His research interests include Earth observation with particular focus on biosphere–atmosphere interactions and ecosystem functioning using imaging spectroscopy.

Mathias Kneubuehler received the M.S. degree in geography and the Ph.D. degree (Dr. sc. nat.) in remote sensing, with emphasis on spectral assessment of crop phenology, from the University of Zürich, Zürich, Switzerland, in 1996 and 2002, respectively.

He is currently leading the Spectroscopy Group, Remote Sensing Laboratories, University of Zürich. His research interests include spectrodirectional data analysis and spectral assessment of phenological processes in vegetated ecosystems.

Daniel Schläpfer (M'10) was born in St. Gallen, Switzerland. He received the M.Sc. degree in geography and the Dr.sc.nat. and Teaching degrees in physics and geography from the Universit of Zürich, Zürich, Switzerland, in 1994, 1998, and 1999, respectively. He received the Teaching Professor degree from the State of St. Gallen, Switzerland, in 2009.

From 1998 to 2008, he was a esearch Scientist with the Remote Sensing Laboratories, University of Zürich. He is currently with the ReSe Applications Schläpfer, Wil, Switzerland and holds a Physics Teaching Position with Kantonsschule, Wil, Switzerland. His research interests include geometric preprocessing of airborne scanner data on the basis of the PARGE software, the application of radiative transfer models in imaging spectroscopy, and the advancement of radiometric and atmospheric compensation in the framework of the ATCOR atmospheric correction solution.

Michael E. Schaepman (M'05–SM'07) received the M.Sc. and Ph.D. degrees in geography from the University of Zurich (UZH), Zurich, Switzerland, in 1993 and 1998, respectively.

In 1999, he was a Postdoctoral Researcher with the Optical Sciences Center, University of Arizona, Tucson, AZ, USA. In 2000, he was appointed as a Project Manager with the European Space Agency APEX Spectrometer. In 2003, he became the Full Chair of Geoinformation Science and Remote Sensing at Wageningen University, Wageningen, The Netherlands. In 2009, he was appointed as the Full Chair of Remote Sensing, UZH, where he is currently heading the Remote Sensing Laboratories, Department of Geography. He is the Director of the University Research Priority Program "Global Change and Biodiversity" and the Vice Dean of the Faculty of Science. His research interests include computational Earth sciences using remote sensing and physical models, with particular focus on the land–atmosphere interface using imaging spectroscopy.